NTNU – Trondheim
Norwegian University of
Science and Technology

Parallel Integration of Aligned Carbon Strings in Polymer Matrix: Dielectrophoretic Preparation, Electrical and Electromechanical Characterisation

Marit Ulset Sandsaunet

Master of Science in Physics and Mathematics
Submission date: December 2012
Supervisor: Steinar Raaen, IFY
Co-supervisor: Geir Helgesen, Institutt for Energiteknikk
Matti Knaapila, Institutt for Energiteknikk

Norwegian University of Science and Technology
Department of Physics

Parallel Integration of Aligned Carbon Strings in Polymer Matrix: Dielectrophoretic Preparation, Electrical and Electromechanical Characterisation

Marit Ulset Sandsaunet

December 7, 2012

Project description

Master thesis project at Physics Department, Institute for Energy Technology:

This project is based on earlier research at Institute for Energy Technology (IFE) which is being patented and will be commercialized by the partly IFE-owned company CondAlign AS. The key idea is to make nanostructured, conducting materials based on electric or magnetic field alignment. Since patents have not yet been granted, some details about the materials and the processes cannot be disclosed.

In general, nanostructured composite materials have many interesting properties which may be very different from the properties of the pure host material that may be, e.g., a polymer. The current project focuses on developing and testing conducting polymer-based composites containing nanoparticles that may be used in strain sensor applications. Conducting polymer composites are commonly made by mixing typically 10% by weight, or more, of conducting particles such as silver or carbon nanoparticles (nanotubes, nanocones or "carbon black") into the polymer when it is in liquid phase. After hardening by heat or UV-light, the particles may form a conductive, percolating network throughout the host matrix and thus make the composite conductive. Strain sensors based on percolating networks have already been used on cantilevers for atomic force microscopy (AFM) or chemical sensing. However, a random percolating network will usually not optimize the conductive properties for sensor applications. Better performance and higher sensitivity can be achieved by aligning the filler particles into single conductive wires or fibres by external electromagnetic fields using the method developed at IFE. When such a material is stretched or strained, some of the conductive pathways will break, and the resistivity of the sensor material increases. Similarly, resistivity will decrease on compression.

In the project, the master student will produce/prepare the materials under the guidance of IFE staff. The resistivity and/or impedance (frequency spectrum) of the material will be measured both unloaded and under strain, and the conductive network structure will be visualised, e.g., using optical microscopy, scanning electron microscopy (SEM) or AFM. So far, "single-string" sensors have been produced and tested, and this project will focus on making more advanced, composite designs involving systems of several aligned, conducting strings that make directional strain sensing in two directions possible. Such design may involve specially designed electrode configurations for aligning and probing, and such electrodes can be made in collaboration with researchers at NanoSYD, University of Southern Denmark.

Project advisors at IFE:
Geir Helgesen, senior scientist
Matti Knaapila, scientist

Sammendrag

Carbon-black-partikler (sot) har blitt opplinjert i tråder ved dielektroforesis. Partiklene ble dispergert i Dymax Ultra Light-Weld® 3094 oligomer-blanding, med et partikkelinnhold på 0.1 vol.%. Blandingen ble spredt over tre ulike elektrodekonfigurasjoner laget på glass- og silisiumsubstrat ved bruk av fotolitografi. Opplinjering ble først testet på det gjennomsiktige og solide glassubstratet for bedre visualisering, og deretter utført på det bøyelige silisiumsubstratet. Silisiumsubstratet var dekket med et isolerende silisiumoksid-lag for å hindre kontakt mellom elektrodene og det elektrisk ledende silisiumlaget.

Den første konfigurasjonen besto av spisse elektrodepar, med elektrodene pekende mot hverandre, og med en avstand på 30 eller 100 µm. De to andre konfigurasjonene besto av de samme spisse elektrodeparene organisert i todimensjonalt matriseliknende og radielt mønster, med henholdsvis 8 og 15 par i hver konfigurasjon. Opplinjering av partiklene ble utført med et alternerende elektrisk felt med feltstyrke på 3-9 kV/cm, etterfulgt av fotopolymerisering (UV-herding) av matriksen, for festing av de opplinjerte trådene.

Opplinjering ble oppnådd på alle elektrodekonfigurasjonene, og den mest vellykkede opplinjeringen ble gjort på den radielle 2D-konfigurasjonen av elektrodepar på glassubstrat. Opplinjering ble utført på sju elektrodebrikker av glass med 15 elektrodepar på hver brikke, og tre av disse resulterte i 15 ledende karbontråder av 15 mulige. Elektriske egenskaper ble studert med dc-målinger og ac-impedansspektroskopi av hver av trådene. Motstanden varierte fra 120 kΩ til 5 MΩ for de ledende trådene, med en middelverdi på 1.03 MΩ.

Opplinjering på det bøyelige silisiumsubstratet ble påvirket av kapasitive effekter og modifisering av feltet mellom elektrodespissene, på grunn av det ledende silisiumlaget. Karbontråder ble dannet i området mellom elektrodene, men motstanden var betydelig større enn for trådene på glassubstrat. Elektromekaniske egenskaper ble studert ved bøying av substratet, og endringer i egenskapene ble observert som følge av strekking av trådene. En reduksjon på 80-90 % av strømmen gjennom opplinjerte tråder ble oppnådd med en avbøyning på 35 µm. Dette tilsier at med optimering av opplinjeringsprosedyren, slik at tråder med lavere motstand kan oppnås på silisiumsubstratet, kan endring i motstand måles som funksjon av avbøyning, og de opplinjerte trådene på det radielle 2D-elektrodemønsteret kan potensielt fungere som en trykksensor.

Abstract

Carbon black particles have been aligned into string-like assemblies by dielectrophoresis. Particles were dispersed in Dymax Ultra Light-Weld® 3094 oligomer mixture, with 0.1 vol.% filler content. This mixture was spread over three different electrode configurations made on glass and silicon substrate by photolithography. Alignment was first tested on the see-through and rigid glass substrate for better visualisation, and then performed on the bendable silicon substrate. The silicon substrate was covered by an insulating silicon oxide layer to separate the electrodes from the conducting silicon.

The first configuration consisted of tip-like electrode pairs, with the electrode tips pointing towards each other, with a distance of 30 or 100 μm. The other two electrode configurations consisted of the same tip-like electrode pairs arranged in two-dimensional matrix and radial patterns, with 8 and 15 pairs, respectively. Electric field alignment of carbon black particles was carried out with an alternating electric field with 3-9 kV/cm, followed by photopolymerisation (UV curing) of the matrix, which locks the aligned strings in place.

Alignment was obtained for all electrode patterns, and the most successful alignment was obtained with the radial 2D configuration of electrode pairs on rigid glass substrate. The alignment procedure was applied to seven samples with 15 electrode pairs on each sample, and three of these samples resulted in 15 conducting carbon black strings out of 15 possible. The electrical properties were studied in terms of dc measurements and ac-impedance spectroscopy for each string. The resistance of strings varied from 120 kΩ to 5 MΩ for the conducting strings, with a mean of 1.03 MΩ.

Alignment on the bendable silicon substrate was influenced by capacitive effects and modification of the electric field between the electrode tips, due to the conducting silicon layer. Carbon black strings were formed in the electrode gaps, but the resistance was significantly higher than for the strings on glass substrate. Electromechanical properties were studied by bending the substrate, and changes in properties were observed as a result of straining the carbon black strings. A reduction of 80-90% of the current through the aligned strings was obtained with a deflection of 35 μm. This means that by optimising the alignment procedure so that strings with lower resistance would be obtained on silicon substrate, the change in resistance could be measured as a function of deflection, and the aligned strings on the 2D electrode pattern could potentially work as a strain sensor.

Preface

This thesis is written in collaboration with the Institute for Energy Technology (IFE), as a part of the Master's Degree Programme in Applied Physics and Mathematics at the Norwegian University of Science and Technology. All alignment procedures and microscopy was done at IFE, while electrical and electromechanical characterisation was done at NanoSYD's facilities during my trip to Denmark.

I wish to show my gratitude to my supervisors at IFE, Matti Knaapila and Geir Helgesen, who have given me constructive feedback through several versions of this thesis. They have guided me in the right direction and have patiently sat through meetings and discussions regarding planning and challenges met on the way.

I also want to thank Jakob Kjelstrup-Hansen at the University of Southern Denmark for making the electrode patterns, for welcoming me to his lab in Denmark, and for all help and clarifications during and after my visit.

Finally, I wish to thank Henrik Høyer for sharing his knowledge in the area of electric field alignment, Henrik Mauroy for sharing his computer skills, my supervisor at NTNU, Steinar Raaen, for quick responses, and Espen T. Nordsveen for his support and encouragement.

Marit Ulset Sandsaunet,
December 2012

Contents

List of Figures

Chapter 1

Introduction

Dielectrophoresis is an effect caused by a non-uniform electric field, in which particles in a fluid will be either attracted to or repelled from areas of higher field gradient. This requires that the dielectric properties of the particles differ from those of the surrounding fluid.

The applications of dielectrophoresis covers a large area, ranging from biosensors, cell therapeutics, drug discovery and medical diagnostics to microfluidics, particle filtration and microscopic strain sensors. Industrial applications include mineral separation, micropolishing and manipulation of fluid droplets and micro components. Advances in technology have also made manipulation of nanoparticles possible, leading to more sophisticated devices in sensor technology, with smaller components and improved sensitivities. [1]

The movement of particles caused by the electric field gradient leads to complicated assemblies depending on dielectric properties, particle density and field structure. With specially designed electrode geometries, this can be used for separation of particles with different dielectric properties. Furthermore, particles such as carbon black (CB) will when exposed to an alternating electric field form a network of strings along the direction of the field [2–4]. This means that an alternating voltage applied to electrodes with particles in a fluid between them, will under the right conditions lead to formation of a connecting wire between the electrodes.

In early studies of dielectrophoresis, fluid motion was influencing the dielectrophoretic effect due to thermal effects from the high voltages that was needed [1]. This was solved by reducing the dimensions of the system, since the dielectrophoretic force acting on the particles is proportional to the gradient of the squared field strength, ∇E^2. This has units of $\mathrm{V^2m^{-3}}$, meaning that with shorter distances a lower voltage can be used to obtain the same force. With more advanced techniques in electrode fabrication, such as photo and electron beam lithography, laser ablation and CMOS technology, sufficiently small electrodes can be made to avoid undesired effects from high voltages. [1]

The movement of CB in electric fields have been subject to investigation by several groups earlier, and possibly first demonstrated by Prasse *et al.* [5] in 1998. This group applied a static electric field to carbon particles in epoxy resin, where

alignment occurs due to the net electric charge on the carbon particles, an effect called *electro*phoresis. They report on a decrease of resistivity by four orders of magnitude after alignment of particles of 0.12 vol.%, compared to a purely homogeneous filler content, due to formation of a percolating network between the electrodes.

The same group also investigated CB-epoxy composites with alternating electric fields with a range of different volume fractions [6]. In this case the system was not aligned. They outline a percolation theory that predicts a percolation threshold, i.e. a lowest particle fraction at which conducting networks of particles form through the matrix, of 16 vol.% for randomly dispersed fillers. As verified by their experiments, the situation with CB in a polymer matrix is more complex than what the theory predicts. The group observed a jump in the conductivity when the particle fraction exceeded 0.9 vol.%, a value which is far below the theoretical value of 16 vol.%. This can be explained by the net electric charge on the carbon particles, which gives particle-particle interactions, and also particle-matrix interactions.

The competing forces at play are the repulsive $1/r$ Coulomb force and contact repulsion, as well as the attractive van der Waals potential, which for point-like particles is proportional to $1/r^6$, as seen in figure 1.1 [6]. For larger particles like CB, the attractive force will not be as steep as $1/r^6$, but rather $1/r^3$, though the overall effect will be the same. With low particle fractions the particles will move away from each other due to the Coulomb repulsion. With higher fractions the particles are forced closer together, and at a certain point they will be close enough and have sufficient energy to overcome the electrostatic barrier, and the attractive Van der Waals potential will overwin the repulsive potentials. The result is a sharp transition from dispersed to agglomerated state of the particles at ~ 0.9 vol.% [5–7].

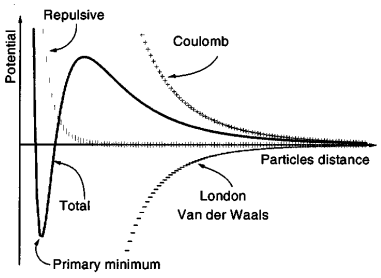

Figure 1.1: Potential energy between particles. Figure reproduced from ref. [6].

In addition to growing carbon wires starting from each of the electrode tips, which will meet on the middle, alternating electric fields can give unidirectional growth of wires, as shown by Sharma *et al.* [8]. They placed carbon nanofibres (CNFs) in epoxy in the area close to one electrode, while the gap between electrodes was filled with plain epoxy. By applying an alternating field, they managed to grow CNF wires as long as 2 cm, extending from one side of the gap to the other. They were also able to grow wires when placing CNFs in the middle of the gap, though more time was needed to complete the wires.

Dielectrophoresis of CNFs have also been studied by Lim *et al.* [9]. Their work showed that when applying an alternating electric field, CNFs assembled in strings through the matrix, working as conducting wires. They report on a decrease in resistivity of three orders of magnitude after electric field alignment of 4.5 wt.% of

CNFs in epoxy.

In recent years there has been an increasing interest in carbon based composite materials in strain sensor applications, and there are several reports on the use of carbon particles as fillers in piezoresistive elements. This includes carbon fibres [10], carbon nanotubes [11–15], isotropic CB [15–18], dielectrophoretically aligned CB [19] and dielectrophoretically aligned carbon nanocones [20].

A device that measures the strain of an object is called a strain gauge, or alternatively a strain sensor. There are today four different categories for commercially available strain sensors; optical, capacitive, piezoelectric and piezoresistive. A piezoresistor exhibits a change in resistance when strained, and this is used to convert strain in terms of vertical displacement to a voltage signal. This has already been done on a wide scale for a variety of applications, e.g. in AFM cantilevers, making a direct readout possible, reducing the sources of error compared to e.g. laser readout, which requires careful alignment and light-to-voltage conversion [17]. Another application is in data storage, where a piezoresistive cantilever can work as a phonograph needle, bouncing up and down over sub-micron indentations on the surface of a polycarbonate disk [21]. The advantage of piezoresistive strain sensors compared to other available sensors are their mechanical stability, their light weight and small size, as well as their high gauge factors [10].

Most piezoresistors today are made of silicon, for different reasons. One is that a thin sheet of silicon returns to its original shape after stretching or bending, a well known behaviour. In addition it is available for both p-type and n-type doping, has a large piezoresistive coefficient and is compatible with high process temperatures, unlike metals. [22]

Gammelgaard *et al.* [17] made a microsized cantilever based on the piezoresistive behaviour of isotropic CB in SU-8 polymer. They used a particle fraction of 16 vol.%, well above the percolation threshold, and reported on gauge factors of 15-20.

Høyer et al. [19] also investigated the possibility for using CB in polymer as a piezoresistor, and added the process of electric field alignment to the procedure. This technology has been patented and commercialised by CondAlign [23]. Moreover, in their study the cantilever, which is fixed in one end only, was replaced by a bridge clamped on both ends and bent on the middle. The alignment of particles allowed for a reduction of the carbon content down to 0.1 vol.%, and a gauge factor of 150 was achieved. With dielectrophoretically aligned particle strings the sensitivity is increased compared to homogeneous fillers, especially for very low strain.

Alignment of rod-like metal particles was pioneered by Smith *et al.* [24]. The idea of using electric field alignment for sensor technology was then investigated by Nocke *et al.* [25], using tellurium nanorods. They achieved a gauge factor of 180. They also mention the use of CB as a homogeneously distributed filler, as done by Gammelgaard *et al.* [17], but claims that with a high filler content the manufacturing process will be strongly limited, especially in the micrometer range.

Burg *et al.* [26] used small band-gap semiconducting single-walled nanotubes (SGS-SWNTs) to make a two-dimensional piezoresistive membrane pressure sensor.

SWNTs were bridged in radially arranged electrode gaps, 19 in total, in a geometric pattern similar to the radial pattern used in this project, shown in figure 3.1c. Of the 19 electrode gaps, 20-30 % resulted in successful depositing of the SWNTs, which is sufficient since only one bridging is required for pressure sensing.

Investigations by Høyer *et al.* [19,27] have shown that when comparing CB and carbon nanocones (CNCs), CB is favourable for making strings in polymer, due to the fact that it is more easily dispersed and has lower production costs. CNCs show higher conductivity when strings are formed, but CB is more likely to form strings in the first place. With this in mind, CB was chosen as material in this project.

CB is an odourless, black powder, most frequently used as a rubber filler [28]. Phenomenologically it is similar to soot and black carbon, but differs in the higher content of elemental carbon, which is usually as high as 97 % for CB. It is low-cost, both compared to CNCs and the increasingly popular carbon nanotubes (CNTs), which have been widely explored for use in sensor technology the last decade. The cost per gram of CB is about 0.1 % of the cost per gram of CNTs (Alfa Aesar) [29].

This thesis presents novel insight into two-dimensional integration of piezoresistive elements, by the combination of two concepts — the aligned carbon strings from Høyer *et al.* [19], and the parallel integration from Burg *et al.* [26]. Alignment on two different two-dimensional electrode patterns are tested, and a detailed analysis of the electrical properties of the aligned CB strings is presented, both on glass and silicon substrate. Alignment on glass substrate is initially optimised on rigid glass substrate for good visualisation, and then moved to silicon substrate for bending analysis. Finally, an approach to strain sensing is made by electromechanical characterisation of the aligned CB strings on silicon substrate, where changes in electrical properties are observed as a function of mechanical deflection.

Chapter 2

Theory

2.1 Dielectrophoresis

The term dielectrophoresis (DEP) comes from the word *dielectric* and the Greek word *phorein*, meaning *to carry*. The term was first used by Pohl in 1951 [30], where he defined dielectrophoresis as "the motion of suspensoid particles relative to that of the solvent resulting from polarisation forces produced by an inhomogeneous electric field."

It differs from the closely related effect *electrophoresis* by the need of a non-zero electric field gradient. Electrophoresis is the movement of a charged dispersed particle relative to the surrounding fluid when placed in a uniform electric field, and is a result of the Coulomb force.

Dielectrophoresis on the other hand does not require charged particles, but particles that exhibit dielectric properties. When the polarisability of the particle is greater than that of the surrounding fluid, the particle will experience a greater force than the fluid, and will move towards areas of greater field strength. The DEP force acting on a spherical particle is given by [1]:

$$F_{\mathrm{DEP}} = 2\pi\varepsilon_m R^3 \mathrm{CM} \nabla |\vec{E}|^2, \tag{2.1}$$

where R is the particle radius, $\mathrm{CM} = (\varepsilon_p - \varepsilon_m)/(\varepsilon_p + 2\varepsilon_m)$ is the Clausius-Mossotti factor, ε_m and ε_p is the absolute permittivity ($\varepsilon_r \varepsilon_0$) of the surrounding medium and the particle, respectivily, and E is the electric field strength. From the equation it is evident that the DEP force is zero for a homogeneous electric field ($\nabla E = 0$). The R^3 dependence tells us that the force will be greater for larger particles, and the E^2 term shows that both ac and dc fields can be used to obtain the effect.

The dipoles can either be aligned or anti-aligned with the electric field, corresponding to a positive or negative force. A positive force will cause the dipoles to move towards areas of higher field strength, while a negative force will cause movement in the opposite direction. This is determined by the sign of the Clausius-Mossotti factor, which will be positive if the particle permittivity is greater than that of the surroundings, and negative otherwise. [1]

To get movement of particles from the dielectrophoretic effect, the DEP force needs to overcome the drag force, F_{drag}, given by Stoke's law:

$$F_{\text{drag}} = 6\pi R\eta v, \tag{2.2}$$

where R is the particle radius, η is the viscosity of the surrounding fluid and v is the velocity. The dielectrophoretic effect will therefore be greater in fluids of higher viscosity. [30]

2.2 Piezoresistance and strain gauge

A piezoresistor undergoes a change in resistance when strained [21]. A measure of the sensitivity of a piezoresistor is the gauge factor K, which is the ratio between relative change in resistance and relative change in length:

$$K = \frac{dR/R}{dL/L}. \tag{2.3}$$

Some common materials and their gauge factors are listed in table 2.1. As shown in the table some materials can have negative gauge factors, meaning that the resistance decreases when the material is strained. This can be achieved e.g. with n-doped silicon, which can give gauge factors down to -125, while p-doped silicon can show gauge factors as high as +200.

Table 2.1: Gauge factors of different materials. Table reproduced from ref. [22].

Material:	Gauge factor:
Metal foil strain gauge	2-5
Thin-film metal	2
Single crystal silicon	-125 to +200
Polysilicon	±30
Thick-film resistors	10

For a circular wire of uniform cross-sectional area, the resistance is given by

$$R = \frac{\rho L}{A} = \frac{4\rho L}{\pi D^2}, \tag{2.4}$$

where ρ is the resistivity of the medium, L is the length, A is the cross-sectional area and D is the diameter of the wire.

In the situation where a small number of microscopic particles are aligned in a wire, the expression for the resistance will be more complex than equation 2.4. The change in resistance due to strain of a string made up of carbon particles aligned in a row, is due to the fact that particles in contact will separate slightly when the string is bent, as shown in figure 2.1, and not as a result of change in the cross-sectional area.

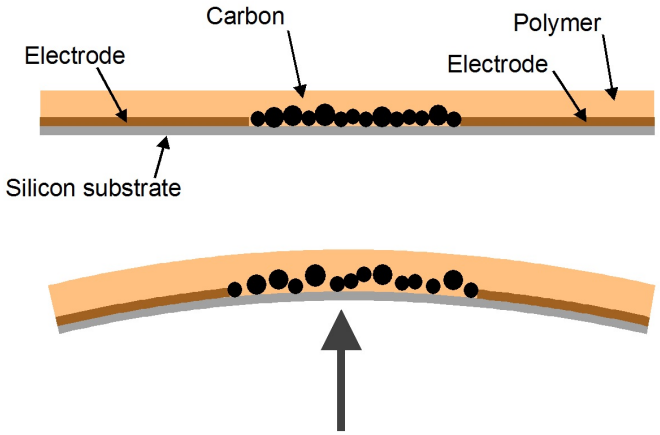

Figure 2.1: Side view schematic of sample during bending. When the substrate is bent, some connections between the CB particles are lost, and the conductance is reduced.

Nocke *et al.* [25] carried out alignment on tellurium nanorods and measured the change in resistance as a result of stretching. They suggest that the sensitivity is determined by the number of particles (in their case nanorods) in a row between the electrodes. The resistance R depends on the hopping conduction between neighbouring particles. The hopping model assumes that the movement of charge carriers is thermally driven and gives the resistance as:

$$R \propto \exp\left[2\alpha d + \frac{W}{kT}\right], \tag{2.5}$$

where α is the inverse localisation length, d is the distance between particles, W is the activation energy, k is the Boltzmann constant and T is the temperature. This means that when the distance d between neighbouring particles is changed as the sample is strained, the resistance should show exponential characteristics. Thus the gauge factor K will vary with the amount of deflection.

The strain, $\varepsilon = dL/L$, is a function of the cross-sectional area A, the applied force F and Young's modulus E in the following way:

$$\varepsilon = \frac{dL}{L} = \frac{F/A}{E}. \tag{2.6}$$

This means that a large change in resistance requires a small Young's modulus and small dimensional parameters. [21]

When calculating the strain of a transversely loaded beam, a reasonable starting point is the axial strain at height z inside the beam, with a radius of curvature ρ. This is given by [31]:

$$\varepsilon = -\frac{z}{\rho}. \tag{2.7}$$

The reciprocal radius of curvature, $1/\rho$, is equal to the double derivative of the deflection, $w(x)$, as a function of position x along the beam [31]:

$$\frac{1}{\rho} = \frac{d^2}{dx^2} w(x). \tag{2.8}$$

The deflection when clamping the beam at both ends is given by [31]:

$$w(x) = \frac{q}{2EWH^3} x^2 (L^2 - 2Lx + x^2), \tag{2.9}$$

where L, H and W is the length, height and width of the beam, respectively, E is the Young's modulus and q is the load. The deflection at the centre of the beam, D, is equal to $w(L/2)$. Rewriting $w(x)$ to an expression of D instead of the load q, and combining equations 2.7 and 2.8, gives the following expression for the strain on the surface of the beam [32]:

$$\varepsilon(x, D) = -\frac{H}{2} \cdot \frac{16D}{L^4} \cdot (2L^2 - 12Lx + 12x^2). \tag{2.10}$$

By calculating the strain and measuring the change in resistance during deflection, the gauge factor K can be determined.

2.3 Impedance and capacitance

In addition to resistance, one can characterise an electronic component by its impedance and capacitance. The capacitance C is given by

$$C = \frac{Q}{V}, \tag{2.11}$$

where Q is the total charge on each of the capacitive elements in the component, and V is the voltage difference between them. The impedance of a capacitor is given by

$$Z_C = \frac{1}{i\omega C}, \tag{2.12}$$

where $i = \sqrt{-1}$ and ω is the angular frequency of the alternating voltage. Detailed calculations giving the resistance R and capacitance C when connected in series and in parallel are presented in appendix A.

Chapter 3

Experimental

3.1 Material preparations

3.1.1 Carbon black in polymer

The CB particles used in this project were provided by Alfa Aesar [29], and had a room temperature density of approximately 2.0 g/cm^3.

The polymer precursor was Dymax Ultra Light-Weld® 3094 (Dymax Corp.) polyurethane oligomer mixture provided by Lindberg & Lund AS [33]. It has a density of 1.01 - 1.03 g/cm^3, and contains 25-50 % urethane methacrylate oligomer, 15-25 % N, N-dimethylacrylamide, 15-25 % isobornyl acrylate, 10-15 % l-vinylhexahydro-2H-azepin-2-one and 1-5 % photoinitiator. UV curing (photopolymerastion) of the oligomer mixture was done using a BlueWave® 200 spot lamp (Dymax).

Mixing of particles and Dymax was carried out with a magnet stirrer at 160 rpm for at least 30 min, and the particle concentration used for alignment was 0.1 vol.%. The value was chosen so that the density would be substantially lower than the percolation threshold, which for these CBs are estimated to be ∼2 vol% [19].

3.1.2 Dynamic mechanical analysis (DMA) of polymer

One sample of CB 0.1 vol.% and one sample of pure Dymax was prepared and cured, in small sheets of thickness 50 and 80 µm, and width of 4.5 and 6.2 µm, respectively. These were then in turn placed in a DMA Q800 instrument (TA Instruments) at NanoSYDs facilities [34], and the samples were stretched up to 200 µm at a rate of 200 µm/min, and the stress and strain was recorded.

3.2 Alignment setup

3.2.1 Electrode patterns

Electrode patterns were made using photolithograpy at NanoSYD's facilities at the Mads Clausen Institute, University of Southern Denmark [34]. Three different electrode patterns were made and used, shown in figure 3.1.

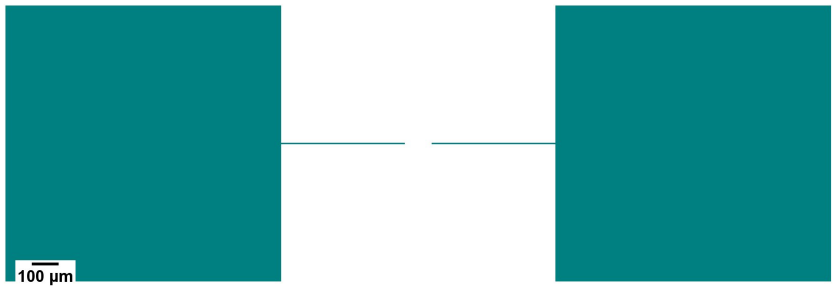

(a) Single electrode pair. The distance between the electrode tips is 100 µm.

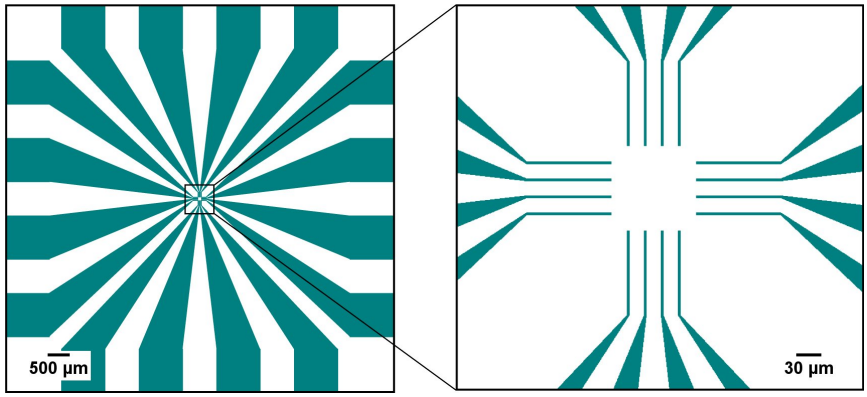

(b) Square electrode configuration. The distance between the electrode tips is 100 µm.

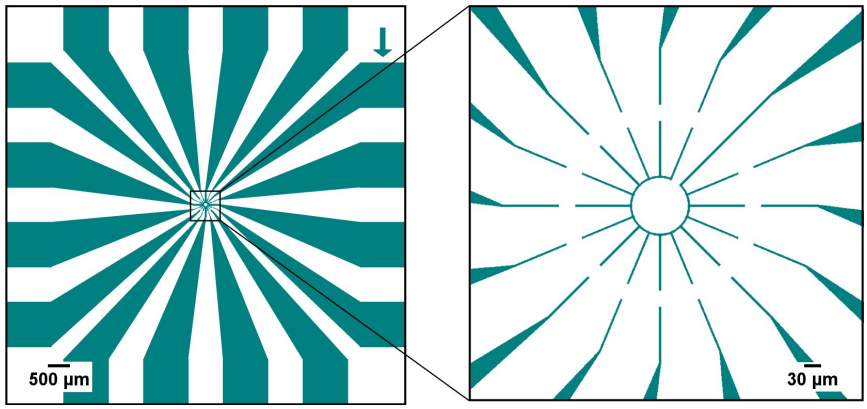

(c) Circular electrode configuration. The distance between the electrode tips is 30 µm. The arrow indicates connection to the inner circular electrode.

Figure 3.1: Schematic showing top view of the electrode patterns made by photolithography. In (b) and (c) the images to the right are magnified selections of the centre part of the images to the left.

The first pattern was a single electrode pair, as shown in figure 3.1a, here with a gap of 100 µm. Experiments were also done using electrode pairs with 30 µm gap.

The second pattern was a matrix configuration of 8 single electrode pairs, where two groups of four electrode pairs were oriented in two directions, which gives a 4 x 4 network of strings, shown in figure 3.1b. The distance between electrodes pointing towards each other was 100 µm.

The third pattern consisted of electrode pairs in a circular configuration, with 15 electrode pairs pointing towards the centre of a circle, as seen in figure 3.1c. The diameter of the circular part of the inner electrode was 100 µm, and the distance between the electrode tips was 30 µm.

3.2.2 Substrate

The electrode patterns were made both on glass and silicon substrate. The glass substrate was 510 µm thick, while the silicon substrate was 150-170 µm thick, and consisted of a layer of silicon followed by an insulating layer of SiO_2, 250 nm thick, on which the electrodes were placed.

At first the electrodes on glass were tested. These were easier to visualise in microscope since the glass substrate was see-through, and so transmission light microscopy could be used. Later on, when the alignment method was optimised on glass, the electrodes on silicon were used, and visualisation was done with reflected light microscopy.

3.3 Electrical alignment procedure

All alignment procedures were done with an alternating voltage at 1 kHz. The field strength was kept at around 3-4 kV/cm. If the mixture contained water impurities, higher field strength could lead to hydrolysis and burning of the sample, while if the field strength was too low the dielectrophoretic effect would diminish. After around 5 minutes with applied field, when the particles were more or less aligned around and between the electrodes, the field strength was increased to as much as 9 kV/cm without causing hydrolysis.

3.3.1 Single electrode pair

The dispersion of 0.1 vol.% CB in Dymax was spread evenly on top of a glass slide with a size of approximately 1 mm x 3 mm, with a single electrode pair as shown in figure 3.1a. The electrode width was 5 µm, and patterns with both 30 and 100 µm distance between electrodes were used. An ac voltage was applied, inducing an electric field between the electrodes.

When the particles were aligned between the electrodes, typically after 5-10 minutes, the sample was cured with UV light for 80 seconds using the BlueWave® 200 spot lamp. The resistance was measured before, during and after the field was applied.

3.3.2 Square electrode pattern

The square electrode pattern was tested on glass substrate only.

CB and Dymax, with a CB density of 0.1 vol.%, was spread evenly on the centre part of the chip, covering the part shown to the right in figure 3.1b. The four electrodes to the left were connected together, as was the four electrodes to the right, while the eight perpendicular electrodes (upper and lower) were left floating.

An ac voltage of 30 V was applied between the two sides, resulting in a field strength of 3.0 kV/cm, and left on for 6 minutes. The resistance between the two sides was measured before and during the time the field was switched on.

3.3.3 Circular electrode pattern

CB particles in Dymax, with 0.1 vol.%, were spread evenly on top of the circular pattern, on both glass and silicon substrate, covering the whole middle area as shown to the right in figure 3.1c.

The 15 outer electrodes were connected together, and an alternating voltage was applied between these and the inner electrode, with amplitude varying from 9-11 V, and left on for 6-30 minutes. Disregarding capacitive effects from the conducting layer on the silicon chips, this would give a field strength of 3.0-3.7 kV/cm between the electrodes. After alignment the Dymax oligomer mixture was cured with UV light for 80-120 seconds. Then the connections between each of the 15 outer electrodes were cut, and the individual resistance of all 15 electrode pairs were measured using a Keithley 2000 multimeter.

When aligning particles on silicon substrate, the inner electrodes were in turns connected and disconnected to the conducting backside of the chip during alignment, to modify the electric field between the electrode pairs.

A schematic of the alignment process is shown in figure 3.2.

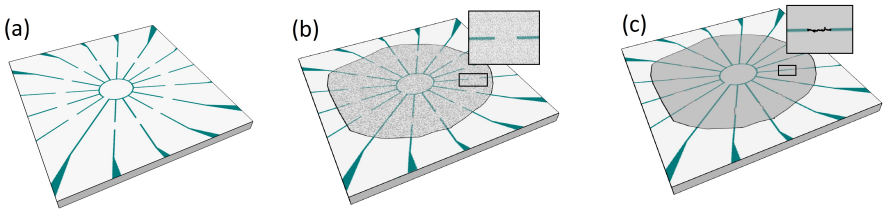

Figure 3.2: Alignment procedure shown with the circular electrode pattern. (a) The electrode pattern on silicon substrate, (b) with CB and oligomer mixture and (c) aligned strings of CB between electrodes after electric field alignment. For clarification the figures are not to scale.

3.4 Electrical and electromechanical characterisation

Electrical properties of samples with aligned 0.1 vol.% CB, isotropic CB with 0.1 vol.% and 12 vol.%, pure polymer and empty electrode chips, all with circular electrode configuration, were characterised.

3.4.1 Instrumentation

Initial electrical characterisation was done with Fluke 179 and Keithley 2000 multimeters. Further electrical and electromechanical characterisation of the samples was performed at NanoSYD's facilities in Denmark [34], using the setup shown in figure 3.3. The silicon chip was held in place by clamps, which was covered in insulating tape to avoid short circuiting. Two tungsten tips controlled by xyz-manipulators were used to connect the electrodes to a Stanford SR830 DSP lock-in amplifier, shown in figure 3.4a, and to a computer with LabView through the Stanford SR570 current preamplifier shown in figure 3.4b.

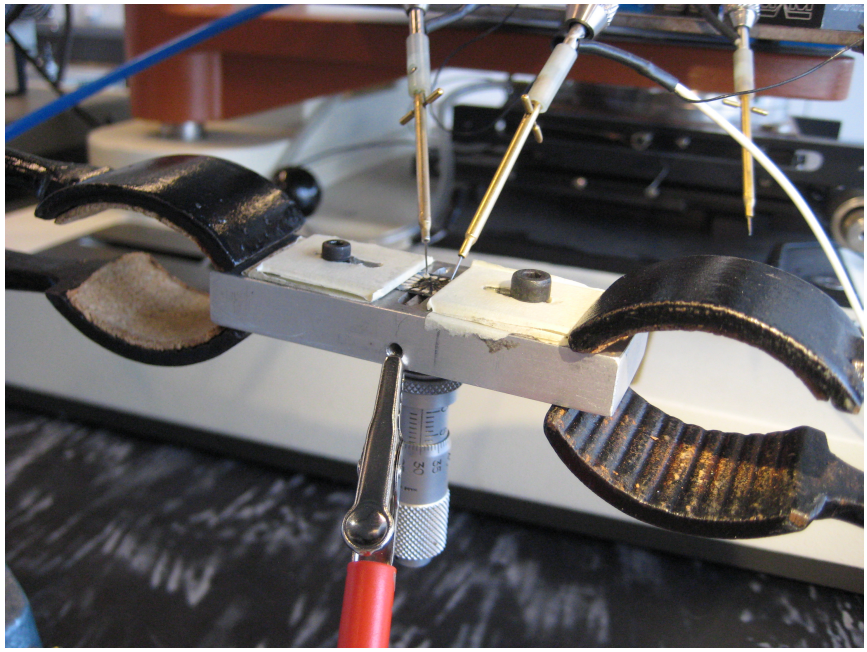

(a) Silicon chip placed with clamps in the holder with a micrometer screw.

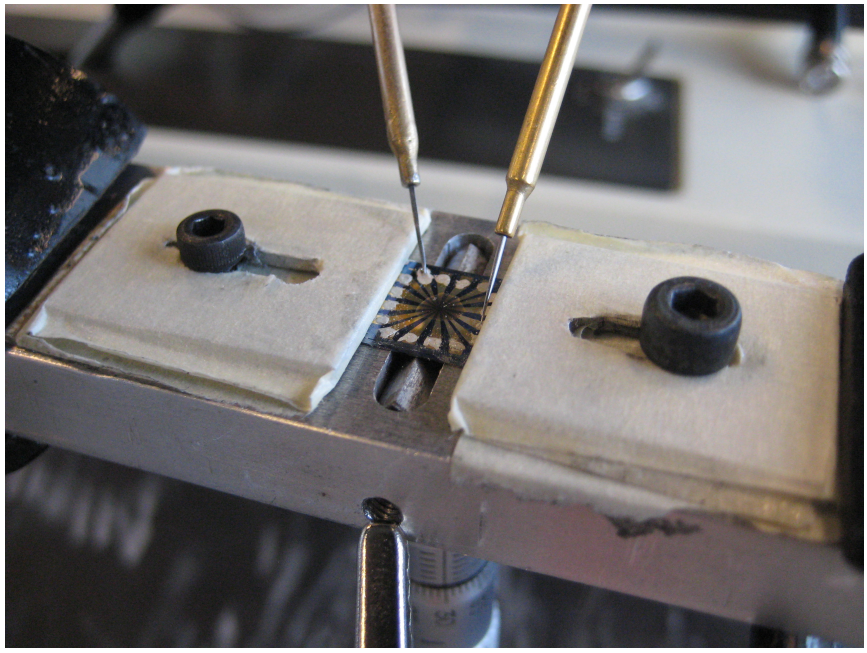

(b) The sample held in place by clamps covered in insulating tape. Tungsten tips were in turn connected to the different electrodes, and data was gathered using instruments shown in figure 3.4

Figure 3.3: Experimental setup for bending measurements.

(a) Stanford SR830 DSP lock-in amplifier used to measure current and phase angle through the samples.

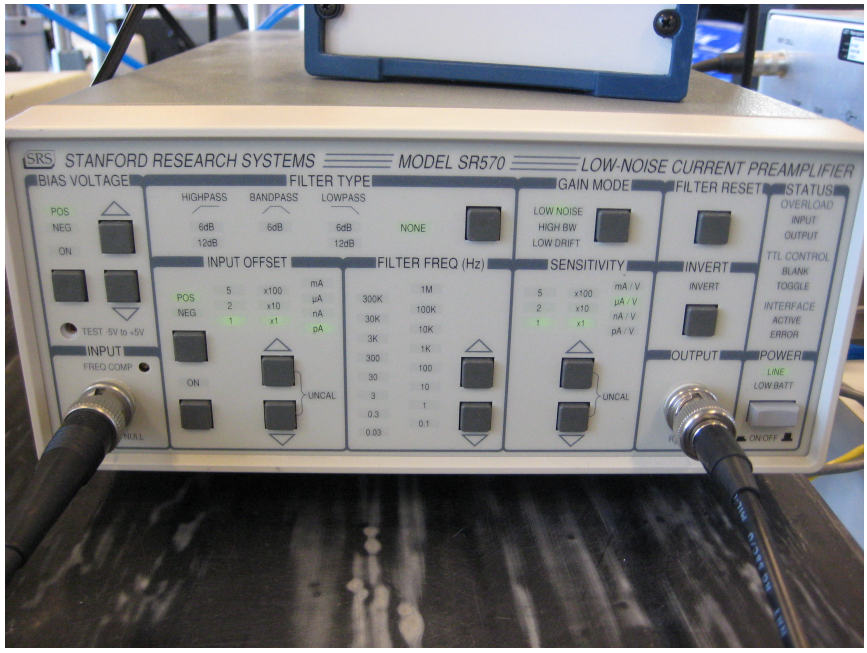

(b) Stanford SR570 current preamplifier, connected to a computer with LabView.

Figure 3.4: Instrumental setup for electrical and electromechanical characterisation of the aligned CB strings.

3.4.2 IV characterisation

A computer with LabView installed was connected to a NI PCI6229 DAQ device, and a LabView program was used to sweep the voltage through the sample from zero to 0.5 V and back again while recording the current. The source current was measured with the SR570 current amplifier connected to the DAQ card.

3.4.3 Impedance and phase angle measurements

Each of the electrode pairs, both on silicon and glass substrate, were in turn connected to the lock-in amplifier in figure 3.4a via the tungsten tips shown in figure 3.3. An ac voltage of 10 or 100 mV at difference frequencies was applied, and values for the current and phase angle were measured. To avoid capacitive effects from the backside of the silicon chip, the backside was grounded through the metal holder.

3.4.4 Strain measurements

Electromechanical characterisation of the strings were carried out by bending the substrate, as shown in the schematic in figure 3.5, while monitoring the impedance through the strings. The silicon chip was placed on the metal block shown in figure 3.3a, on top of a movable triangular piece of metal with a sharp edge, controlled by a micrometer screw. The edge can be seen underneath the chip in figure 3.3b. The tungsten tips were connected to the inner electrode as well as one electrode perpendicular to the movable edge. The edge was then moved upwards 5 µm at a time, bending the silicon chip, up to 30 - 45 µm, while impedance and phase angle, as well as IV-curves, were measured for each displacement.

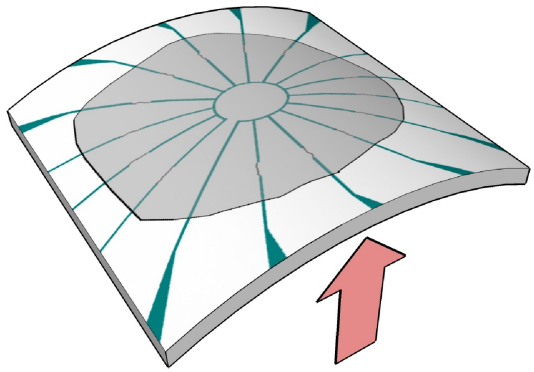

Figure 3.5: Bending of substrate with aligned strings. For clarification the figure is not to scale.

Chapter 4

Results

4.1 Materials

Figure 4.1 shows 0.1 vol.% CB in oligomer mixture after 2 days and 5 weeks of stirring at 160 rpm. The particles are more evenly dispersed after 5 weeks.

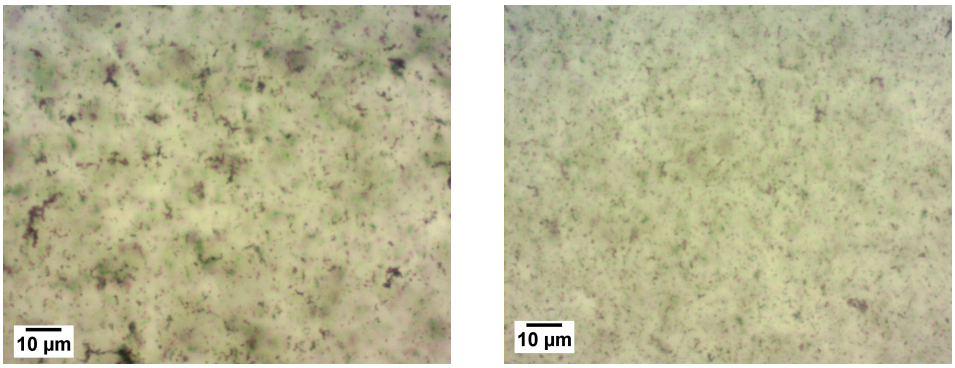

(a) **(b)**

Figure 4.1: CB 0.1 vol.% after (a) 2 days and (b) 5 weeks.

4.1.1 Dynamic mechanical analysis

Figure 4.2 shows the stress-strain curves from the DMA testing of polymer and 0.1 vol.% CB. The Young's modulus for both samples has been estimated from the slope of the initial linear part of the stress-strain curves, and found to be 47 MPa for pure polymer and 25 MPa for CB 0.1 vol%. The value from the manufacturer of the polymer (Dymax) is 240 MPa. The estimated values show that the elasticity is reduced to nearly 50 % when adding a filler content of 0.1 vol.%.

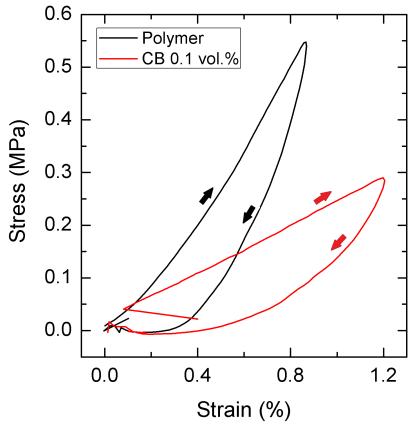

Figure 4.2: Stress vs. strain from dynamic mechanical analysis (DMA) for pure polymer (Dymax) and 0.1 vol.% CB in polymer, when stretching the sample 200 µm at a rate of 200 µm/min. The arrows indicate direction of displacement.

4.2 Alignment

4.2.1 Single string alignment

When exposed to an alternating electric field, the CB particles aligned in strings between the electrodes, as expected. This is shown in figure 4.3, with the arrangement of particles before field and after 5 min with 4 kV/cm, with an electrode distance of 30 µm. The resistance between the electrodes before alignment was higher than what could be measured with our instrument ($> 100\ \Omega$), and after alignment the resistance was reduced to $\sim 1\ \mathrm{M}\Omega$. When assuming a rough estimate of dimensions of 3 µm x 3 µm x 30 µm for the aligned CB string, this corresponds to a conductivity in the order of a few S/m, which is consistent with previous observations [19].

4.2.2 Square electrode pattern on glass substrate

Before the field was applied, there was no measurable conductance between the electrodes (resistance higher than 100 MΩ). After four minutes of alignment the resistance was reduced to 1.2 MΩ, matching the resistance of aligned single strings. Micrographs taken before and after field is shown in figure 4.4. As can be seen in figure 4.4c, the CB strings from the upper and lower electrodes connected to the perpendicular, floating electrodes, instead of the opposite electrode. Strings from the middle electrodes connected to the opposite side, but also to neighbouring electrodes and not only to the direct opposite ones.

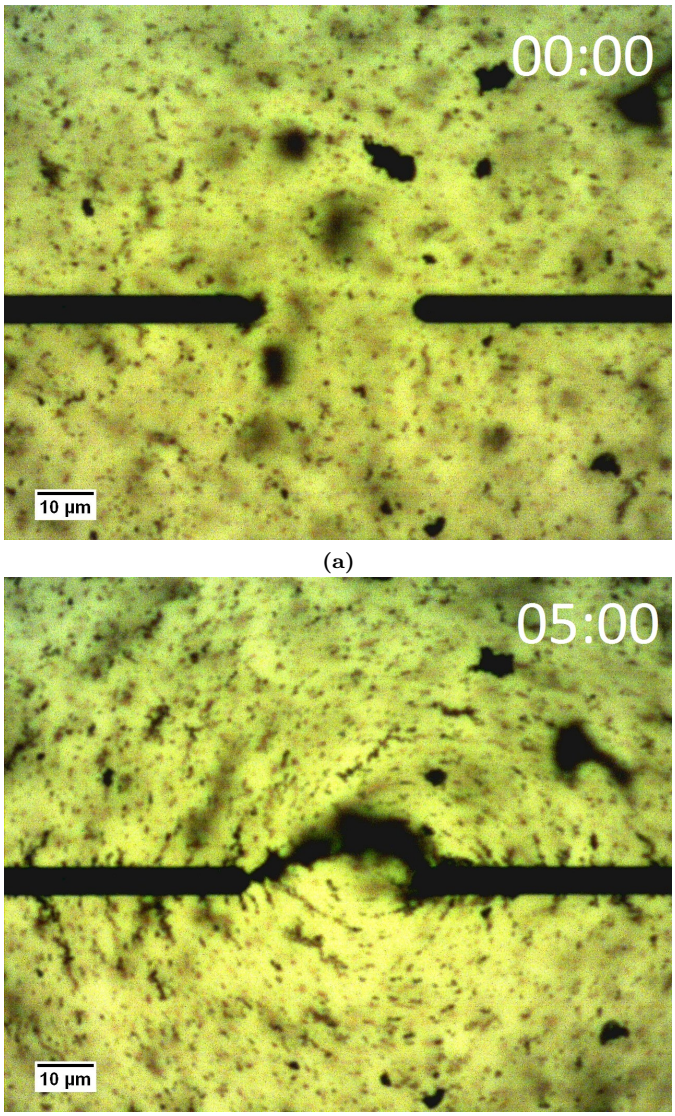

Figure 4.3: CB in Dymax (a) before field and (b) after 5 min with applied field of 4 kV/cm. The distance between the electrodes is 30 µm, and the final resistance was measured to be approximately 1 MΩ.

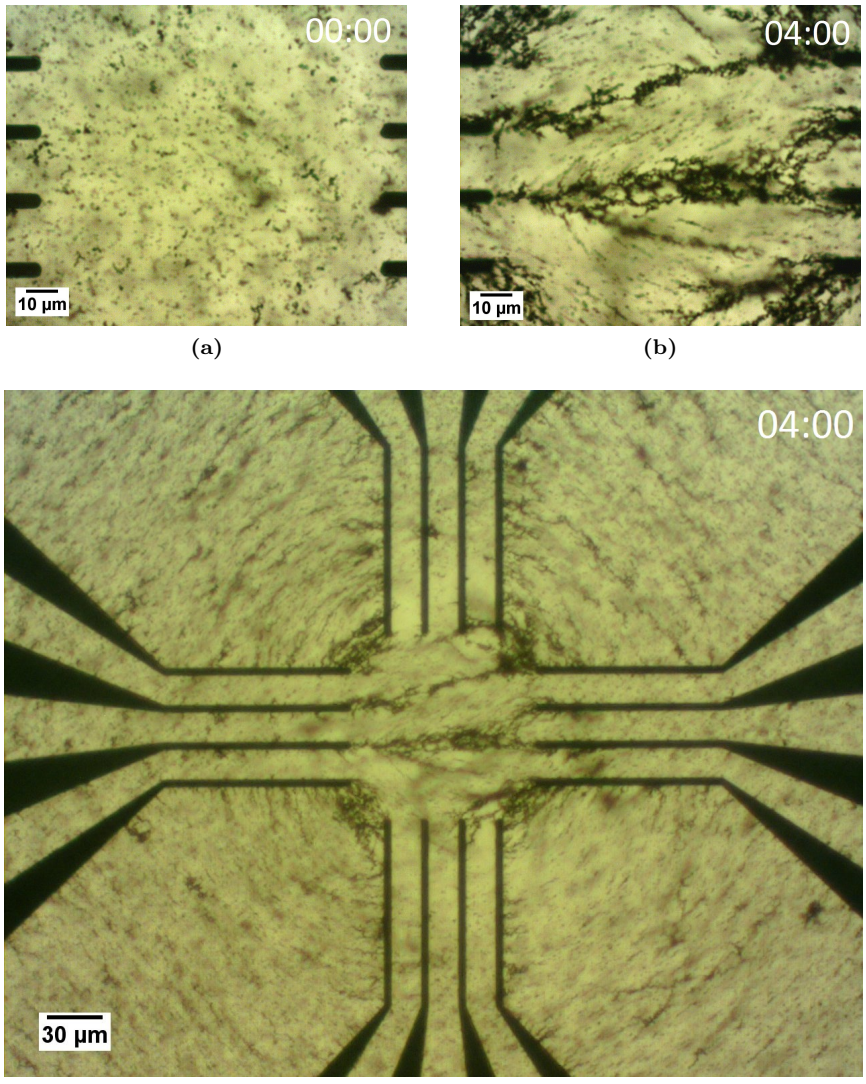

(a) **(b)**

(c)

Figure 4.4: CB on square electrode pattern (a) before and (b),(c) after 4 minutes with 3 kV/cm. The four electrodes to the left and the four to the right were connected together, while the perpendicular electrodes were left floating. The distance between opposite electrodes is 100 µm.

4.2.3 Circular electrode pattern on glass substrate

Figure 4.5 shows a photo of a glass chip with circular electrode pattern, with polymer with 0.1 vol.% CB covering the centre part. Before the field was applied, the resistance across the electrode gaps was to high to be measured with our instruments (> 100 MΩ). As shown in figure 4.6, CB strings were created between the electrode pairs after 11 minutes with applied field of strength 3.0 - 3.7 kV/cm. Of the seven samples that were tested, three of the samples resulted in 15 conducting strings out of 15 possible, with resistances of 0.12 - 5 MΩ, while the other samples gave only a few conducting strings. Figure 4.7 shows micrographs of all 15 CB strings from figure 4.6d, where all strings were conducting.

The difference between a conducting and non-conducting string is difficult to observe by visual inspection, as seen in figure 4.8, where micrographs of a conducting string with 1 MΩ resistance and a non-conducting string is shown.

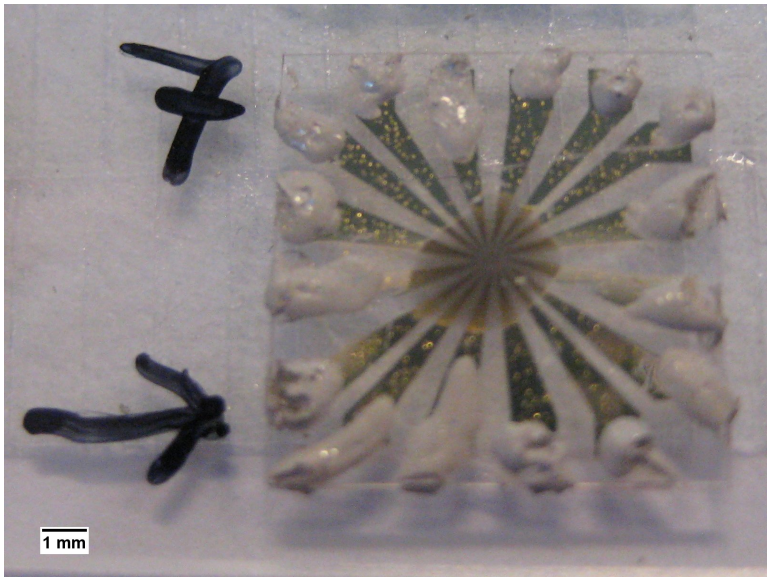

Figure 4.5: Glass chip with circular electrode configuration. The dark spot in the centre of the chip shows the 0.1 vol.% CB. The arrow indicates contact to the inner electrode.

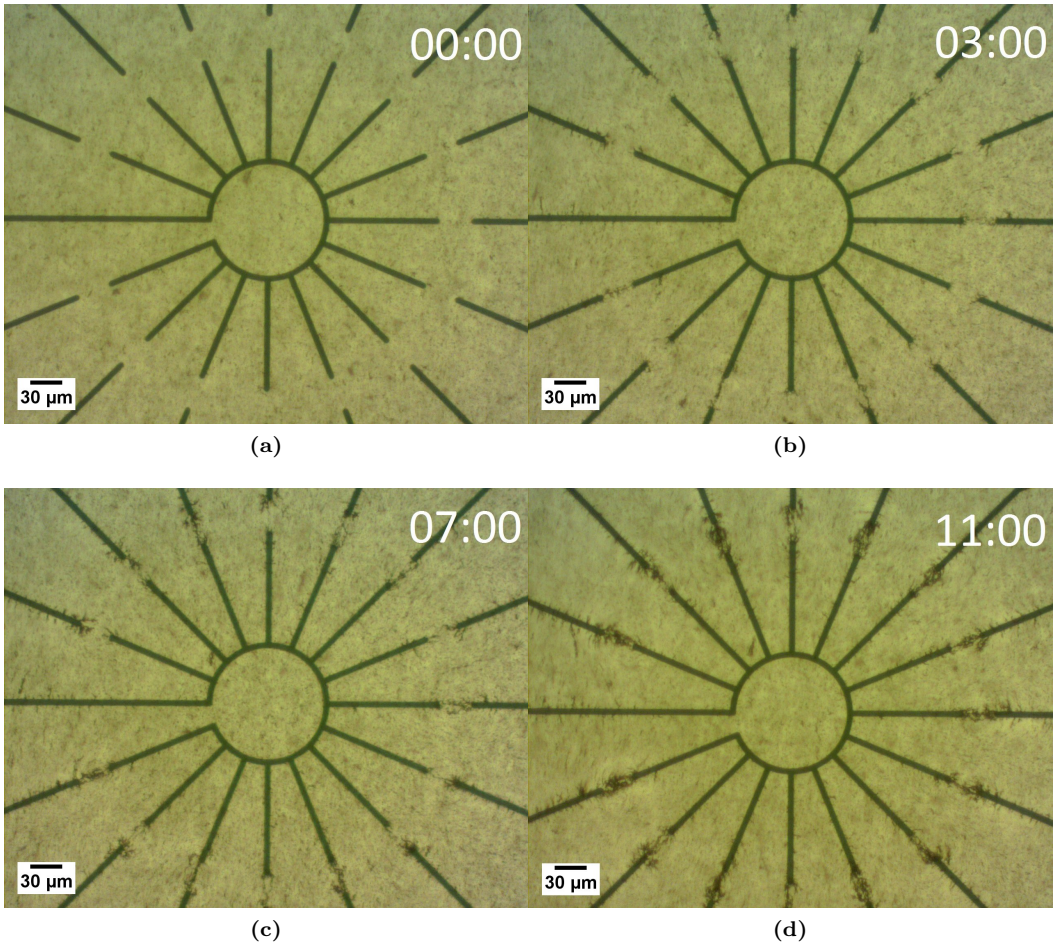

(a) **(b)**

(c) **(d)**

Figure 4.6: CB on circular electrode pattern on glass substrate (a) before field, and after 3 (b), 7 (c) and 11 (d) minutes with 3.0 - 3.7 kV/cm. The inner circular electrodes is connected through the electrode pointing towards left.

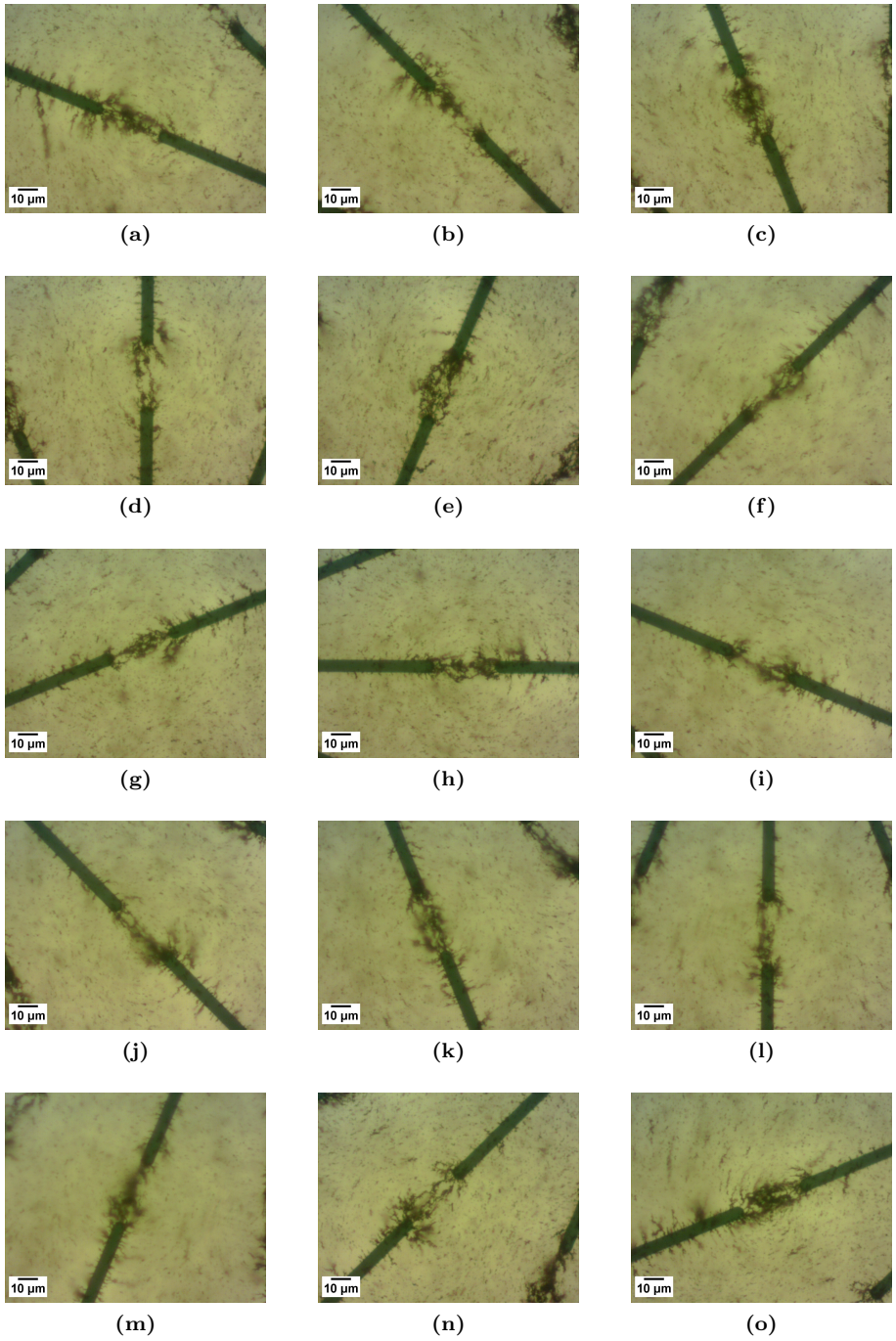

Figure 4.7: CB on glass substrate with electrodes in circular configuration, with applied field of 3.0-3.7 kV/cm for 11 min, showing each of the CB strings. The distance between the electrodes is 30 µm. The order of the electrode pairs is clockwise around the circular geometry, starting to the right of the inner electrode connection.

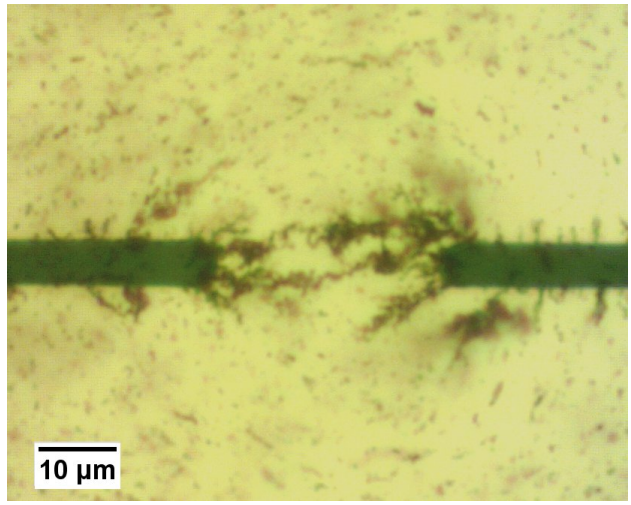

(a)

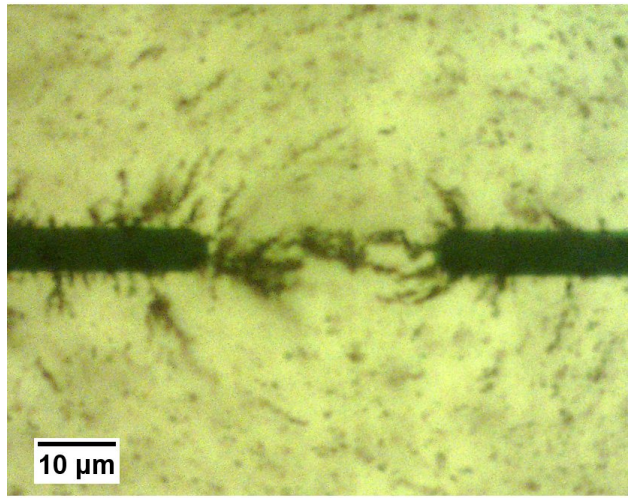

(b)

Figure 4.8: Micrographs showing (a) a conductive CB string with resistance of 1 MΩ and (b) a non-conductive string, both on glass substrate. The distance between electrodes is 30 µm, and both electrode pairs shown here were part of a circular configuration as shown in figure 3.1c.

4.2.4 Circular electrode pattern on silicon substrate

Electric field

When a voltage was applied to the electrodes, an electric field was induced around and between the electrodes. A simulation of the electrical field lines was done using a simple software (Electric Field 2.01 [35]). In the software positive and negative charges could be positioned in different patterns, and electric field lines were then calculated and visualised.

The result from the simulations are shown in figure 4.9. The figure shows a simplified model of the instantaneous charge distribution on the silicon chip, with the inner and outer electrodes, as well as the conducting backside layer of the chip. Figure 4.9a shows the field lines between two oppositely charged electrodes. In figure 4.9b the charge on the electrodes have induced a charge distribution on the conducting backside, reducing the field strength between the electrodes. Figure 4.9c shows the backside when it is connected to the inner electrode, while in figure 4.9d the backside is connected to the outer electrodes. Figure 4.9e shows a simplified model of the electrode pattern seen from the top (dimensions and number of electrodes are not to scale).

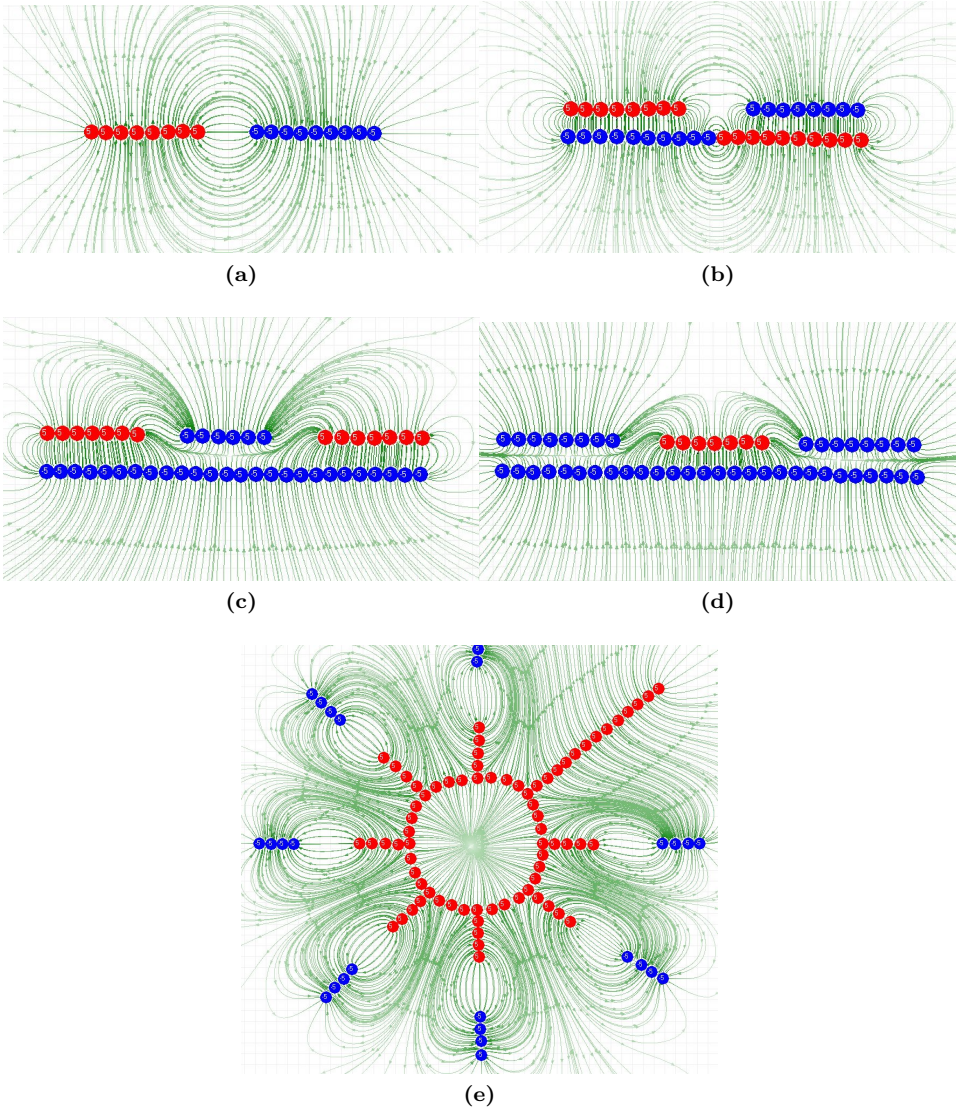

Figure 4.9: Model of the instantaneous charge distribution (a) between two oppositely charged electrodes, (b) with a conducting layer underneath the electrodes, (c) a very simple model of a silicon chip seen from the side with the backside connected to the inner electrode, (d) simple model seen from the side with the backside connected to the outer electrodes and (e) the electrode pattern seen from the top. Dimensions and number of electrodes are not to scale.

Alignment with circular electrode pattern on silicon substrate

Figure 4.10 shows a photo of a silicon chip with circular electrode pattern, with 0.1 vol.% CB in the centre. Figure 4.11 shows the alignment process of 0.1 vol.% CB from 0 to 19 minutes with 3 - 5 kV/cm with circular pattern on silicon substrate.

Particles build up in the gap between electrodes, and by visual inspection all the strings look intact. However, only one of these strings was conducting, with a resistance of 2.8 MΩ, while the rest had a resistance from 8 MΩ to more than 100 MΩ (the highest resistance that could be measured with our instruments). Figure 4.12 shows micrographs of each of the strings from figure 4.11d, where 4.12n shows the conducting string.

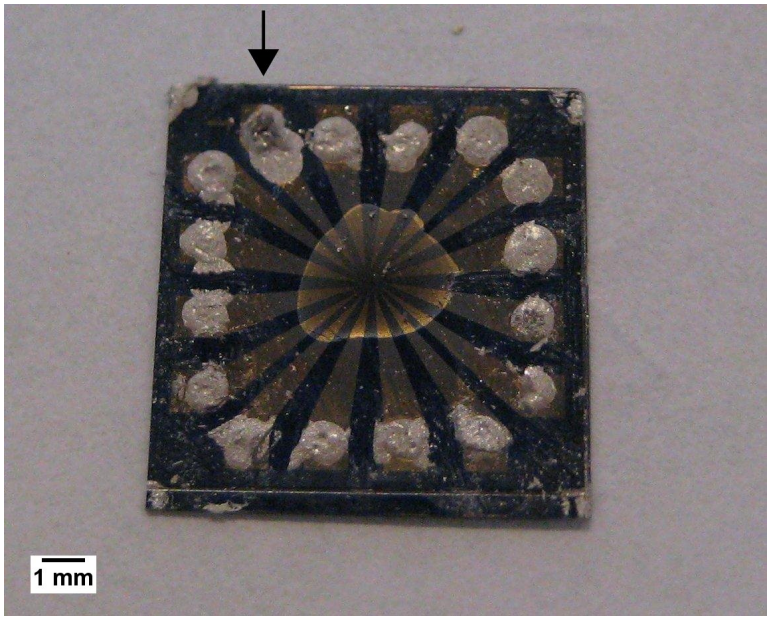

Figure 4.10: Silicon chip with circular electrode configuration. The 0.1 vol.% CB is visible in the centre of the chip, and the arrow indicates the connection to the circular inner electrode.

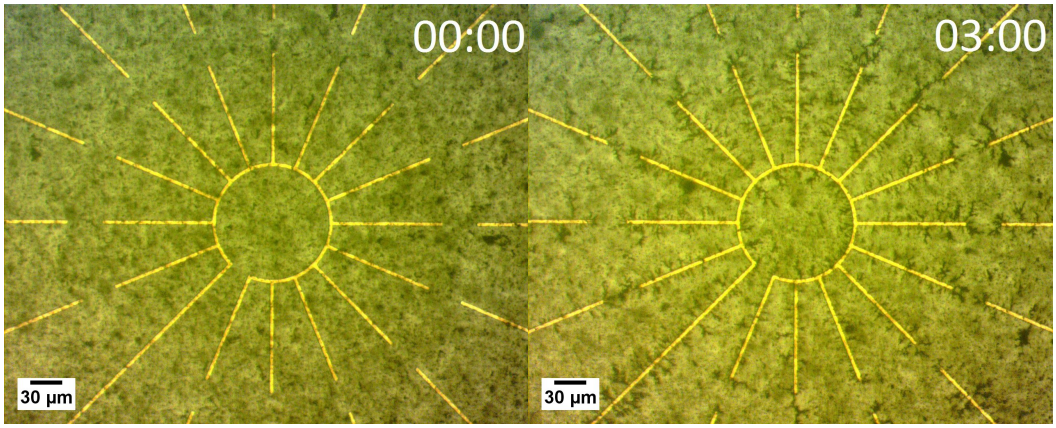

(a) (b)

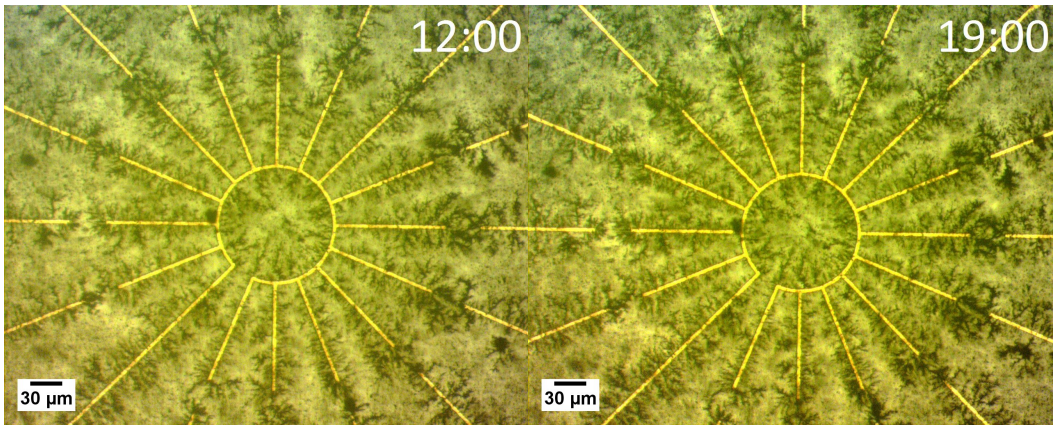

(c) (d)

Figure 4.11: CB 0.1 vol.% on circular electrode pattern on silicon substrate (a) before field, (b) after 3 minutes, (c) after 12 minutes and (d) after 19 minutes with 3 - 5 kV/cm.

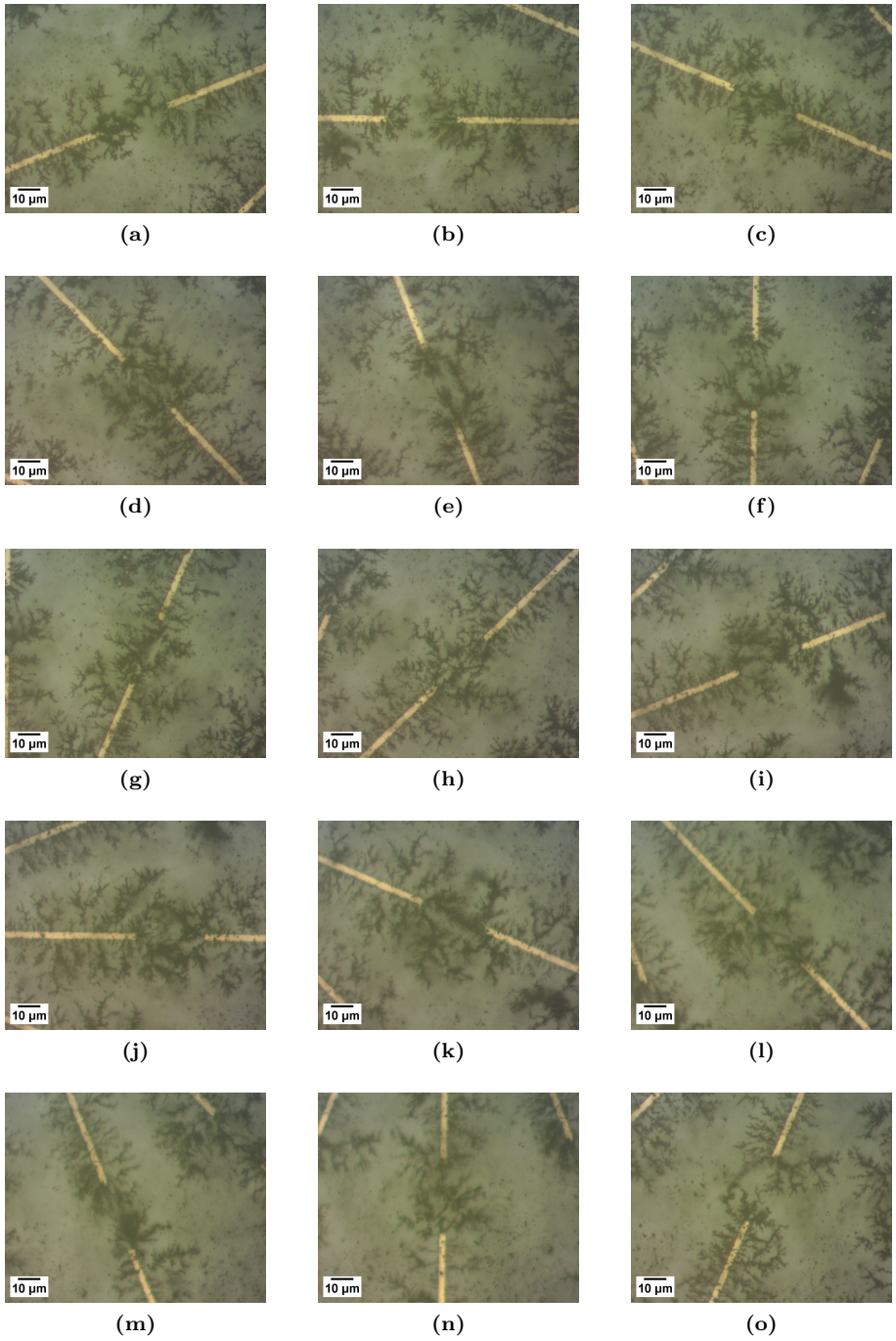

Figure 4.12: Micrographs of each of the CB strings in figure 4.11d. The distance between the electrodes is 30 µm. The order of the electrode pairs is clockwise around the circular geometry, starting to the right of the inner electrode connection.

4.3 Characterisation

4.3.1 Resistance on glass substrate

A complete analysis of single strings has been done previously by Høyer *et al.* [19, 27], so the focus in this thesis is on the behaviour of these strings when placed in two-dimensional arrangements. Detailed characterisation was done for strings on the circular electrode pattern only, due to the more successful results for these than for the square pattern.

The electrical properties of 7 samples, giving 105 strings in total, were analysed. All together 65 % of the strings on glass substrate had a resistance value lower than 5 MΩ, when measured with a Keithley 2000 multimeter. The distribution of these are shown in the histogram in figure 4.13. The resistance of strings varied from 120 kΩ to 5 MΩ for the conducting strings, with a mean of 1.03 MΩ.

Three of the seven samples had 15 out of 15 conducting strings, while the rest had only a few conducting strings. Figure 4.14a shows an example of an IV-curve of one of the conducting strings. As seen from this example, the IV-curves were both linear and reversible upon cycling, meaning that the system was ohmic. Hence, the resistances could be calculated from linear fits of the IV-curves, and the results from this are shown in figure 4.14b. Here the resistance of 15 CB strings on the same glass chip is shown. The figure also shows resistance for the same strings calculated from ac impedance measurements by extrapolating data down to zero frequency.

The resistance was measured again 3 and 10 weeks after alignment, and graphs showing the change in resistance and the relative change in resistance are shown in figure 4.15a and 4.15b, respectively. Data in figure 4.13 is gathered from 68 strings, while data in figures 4.15a and 4.15b is gathered from 30 strings, all with resistance lower than 5 MΩ.

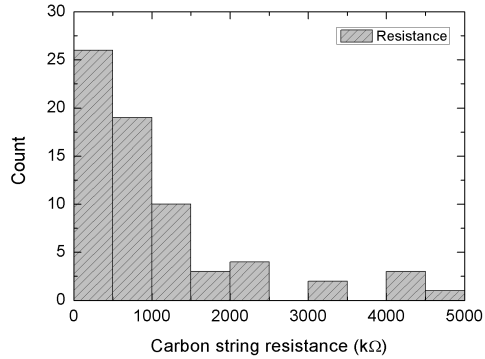

Figure 4.13: Histogram for resistance for CB strings on glass substrate.

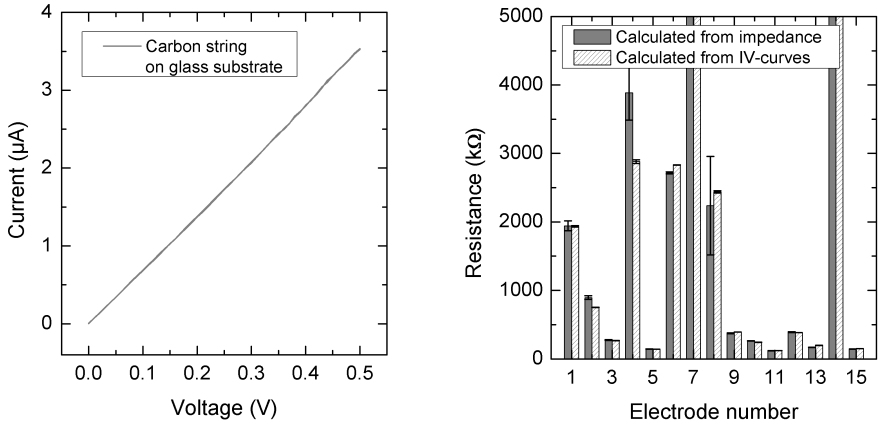

(a) **(b)**

Figure 4.14: (a) IV-curve for a string on glass substrate. (b) Histogram showing the resistance for strings on glass substrate calculated from impedance and IV-curves.

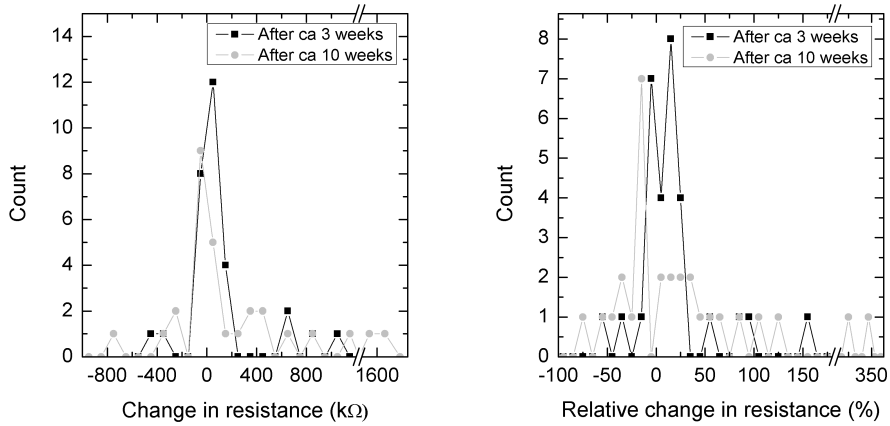

(a) **(b)**

Figure 4.15: (a) Change and (b) relative change in CB string resistance 3 and 10 weeks after alignment, measured with a Keithley 2000 multimeter.

4.3.2 IV characterisation

Values for the current through the samples were recorded while the voltage was sweeped from zero to 0.5 V and back to zero. Figure 4.16a shows IV-curves for conducting strings on glass substrate, as well as background (lowest curve, in black). The string resistances calculated from linear fits range from 120 kΩ - 9.4 MΩ. Figure 4.16b shows IV-curves for one aligned string on glass substrate, and for one aligned string and background on silicon substrate. The current was basically equal to zero for the samples on silicon, while the linear fit for the CB string on glass gave a resistance of 2.9 MΩ.

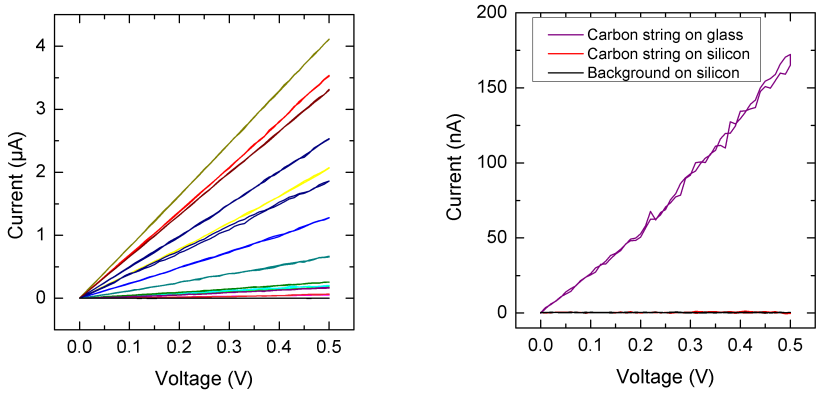

(a) **(b)**

Figure 4.16: (a) Current as a function of voltage for 15 aligned strings on the same glass substrate, where the voltage was sweeped from zero to 0.5 V and back to zero (loop). The black line (lowest IV-curve) shows the background on glass substrate. (b) Comparison of current as a function of voltage between aligned CB strings on glass and silicon substrate, also showing background signal on silicon substrate. The current for the string and background on silicon is basically equal to zero, and the curve for the string on glass substrate corresponds to the purple curve in (a) (third curve from bottom).

4.3.3 Impedance and phase angle measurements

Impedance and phase angle was measured for all samples, and the results for aligned strings on glass substrate, where all 15 strings were conducting, are shown in figure 4.17. Impedance was found by dividing the voltage amplitude with the absolute value of the current. The results show that the impedance and phase angle is fairly stable for low frequencies. Figure 4.18 shows impedance and phase angle for one aligned CB string on silicon substrate, in addition to results for empty electrode pattern, isotropic CB with 0.1 vol.% and 12.0 vol.% and pure polymer (Dymax) for comparison. The applied voltage was 10 mV for 12 vol.% CB, and 100 mV for the rest of the samples. Values from the whole scale of frequencies were gathered both for glass and silicon substrate, but only values where the current was lower than 1 μA is included.

The instrument for measuring current and phase angle was controlled with standard electrical components with known phase angle, to ensure validity of the measured values.

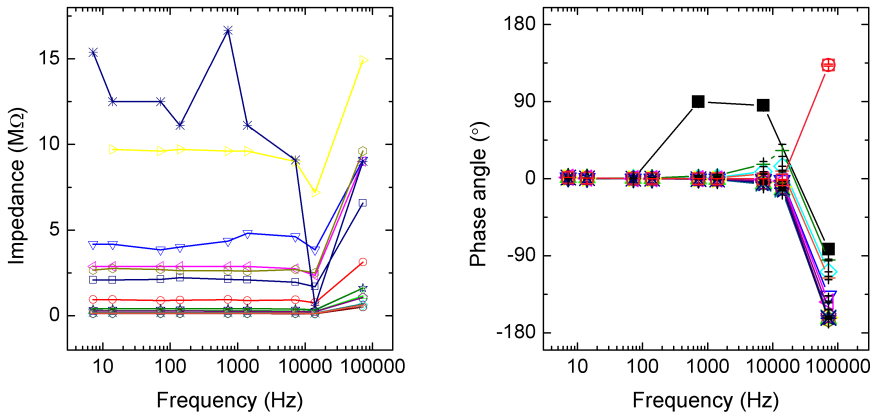

Figure 4.17: (a) Impedance and (b) phase angle as a function of frequency for strings on glass substrate with circular electrode pattern, where all 15 strings were conducting. Each symbol corresponds to a different CB string, and the applied voltage was 100 mV. In (b) the black squares show the phase angle for the empty electrode pattern.

4.3.4 Strain measurements

Silicon chips with aligned strings were deflected using a movable triangular piece of metal controlled by a micrometer screw, while values for current and phase angle were recorded. The applied ac voltage was 10 mV at 14 kHz for the isotropic 12 vol.% CB, and 100 mV at 1.4 kHz for the other samples. The chips with the CB

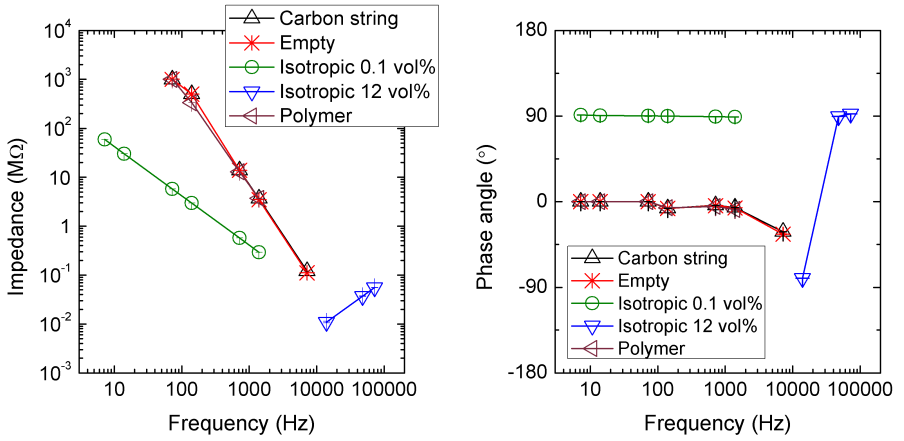

Figure 4.18: (a) Impedance and (b) phase angle as a function of frequency on silicon substrate with circular electrode pattern, for aligned CB string, empty electrode pattern, isotropic CB with 0.1 vol.% and 12.0 vol.%, and pure polymer (Dymax). The applied voltage was 10 mV for 12 vol.% CB, and 100 mV for the rest of the samples.

string and the 12 vol.% dispersion broke at the highest point of deflection, and so there is no data for going back to zero deflection.

Strain was calculated both from equation 2.10 and using the computational software COMSOL [32]. Both calculations are plotted in figure 4.19, which shows that equation 2.10 gives a good approximation for small deflections. Typical values for L, H and x were 9 mm, 150 µm and 4.665 mm, respectively.

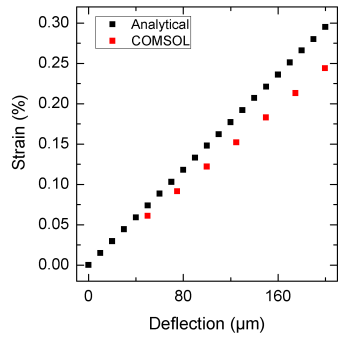

Figure 4.19: Calculated strain using equation 2.10 and the computational software COMSOL.

Figures 4.20a and 4.20b show the resulting current and phase angle as a function of deflection for one aligned CB string, isotropic CB with 0.1 vol.% and 12.0 vol.% and pure polymer (Dymax). The top axis shows the corresponding strain from the analytical calculation.

Figure 4.20c shows the current as a function of deflection for two CB strings on different silicon chips. While one chip broke on the highest point of deflection (the same as in figures (a), (b) and (c)), the other shows the return to zero deflection. The current through the aligned strings is significantly influenced by deflection, while isotropic samples show a much smaller relative effect.

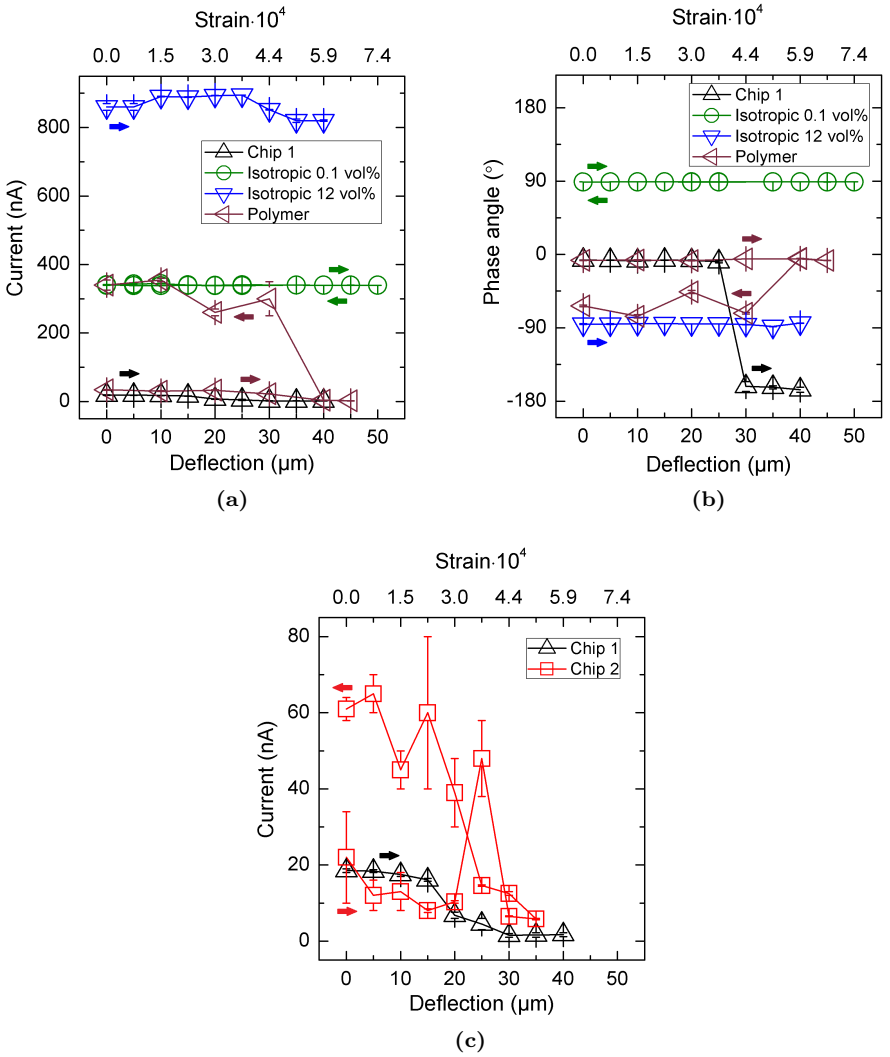

Figure 4.20: (a) Current and (b) phase angle as a function of deflection on circular electrode pattern for aligned string (Chip 1), isotropic CB with 0.1 vol.% and 12.0 vol.% and pure polymer (Dymax). (c) Comparison of current as a function of deflection for the same aligned string as in (a) and (b) (Chip 1), with an aligned string on a different silicon chip (Chip 2). The applied voltage for 12 vol.% isotropic CB was 10 mV at 14 kHz, while for the rest of the samples it was 100 mV at 1.4 kHz. Arrows indicate direction of deflection.

Chapter 5

Discussion

5.1 Materials

CB particles were dispersed in a UV curable Dymax oligomer mixture before electric field alignment was carried out. Figure 4.1 shows micrographs of 0.1 vol.% CB in Dymax after 2 days and after 5 weeks of stirring with a magnet stirrer at 160 rpm. After 2 days the dispersion still contains some large aggregates, while after 5 weeks of stirring the particles are well dispersed. This indicates that the mixing should be done for more than 2 days to obtain a better dispersion.

A dynamic mechanical analysis was performed on UV cured Dymax to determine the elastic properties of the polymer, both for Dymax containing 0.1 vol.% CB and for pure polymer. Figure 4.2 shows the stress versus strain for these two samples. The reduction in Young's modulus, i.e. the reduction in the initial slope of the curve, resulting from adding CB shows that the polymer stiffness is altered by the filler. This, and the larger hysteresis with filler compared to pure polymer, shows that it is advantageous to have a lowest possible filler content.

The estimated values of the Young's modulus for pure polymer from the DMA measurements was about 20 % of the manufacturers value. The thickness used when estimating the Young's modulus by the manufacturer is not know, and so a difference in thickness and shape can be the reason for the large deviation. Another explanation could be that the difference is a result of the curing process. The curing of these samples was done using hand-held UV sources at a non-fixed distance, which might not lead to a uniform and complete curing.

An attempt was made to make a DMA sample with 12 vol.% CB as well, but because of the high filler content it was hard to cure the sample properly.

5.2 Alignment

Two different two-dimensional electrode configurations were tested in this project — a radial configuration with 15 electrode pairs oriented in a circle, and a square

configuration where four and four electrode pairs were placed perpendicular to each other, which ideally would result in a 4 x 4 network of strings.

With the square configuration the alternating voltage was applied to electrode pairs in one direction only, while the perpendicular electrodes were left floating. During the alignment the floating electrodes modified the electric field, so that CB particles assembled between one electrode and the closest floating electrode. This effect could be eliminated by only applying the CB dispersion to the area of interest, i.e. to cover up the floating electrodes. Then the particles would not have the possibility to move towards the floating electrodes, and would be more likely to move in the desired direction. Covering up electrodes in one direction was not straight forward, since the area of interest had a width of less than 100 µm, and the electrodes were very fragile, so that covering them up might break them.

The challenges met with alignment of the CB particles on the square configuration, as well as the higher degree of symmetry in the circular configuration, led to the decision of using the circular pattern for future investigations. While the square pattern has only two axes of symmetry, the circular pattern has eight axes of close-to-perfect symmetry. This gives a greater advantage in sensor applications, since strain can be measured in several directions.

The alignment process with the circular electrode pattern was optimised on glass, under good visualisation conditions using transmission light microscopy, and later on transferred to silicon substrate. The silicon substrate could then be used to perform electromechanical characterisation of the aligned CB strings, since the substrate could be bent slightly without breaking.

The choice of using silicon as a substrate was based on accessibility of the material, as well as the fact that the electrodes are easily attached to this substrate. In addition it is a popular choice for sensor applications due to the elastic properties, and it was a natural choice when making comparisons to Gammelgaard *et al.* [17].

Ideally, the elastic properties of the substrate should be similar to those of the studied materials on it, so that the substrate doesn't break before the material does. Therefore, a possibility for the future could be to use an elastomer as a substrate, which usually has a low Young's modulus and more suitable elastic properties than silicon. The challenge with such a substrate would then be to attach the electrodes properly.

Even with well-attached electrodes, optimised alignment procedure and well-dispersed particles in the oligomer mixture, the alignment procedure proved to be more challenging on silicon substrate than on glass. The CB particles seemed to form complete strings by visual inspection in microscope, but resistance measurements showed that nearly all of the strings had a resistance that was too high to be measured. On each of the silicon chips only a few of the strings — at most, showed resistance below 20 MΩ. The main reason for the different results on silicon substrate compared to glass lies in the conducting silicon layer underneath the insulating layer of SiO_2, on which the electrodes are attached. The conductive silicon layer gives capacitive effects and a considerable modification of the electric field between the electrodes when an alternating voltage is applied.

As seen in figures 4.7 and 4.12, where particles are aligned in the electrode gaps

on the circular electrode pattern, the particles on both glass and silicon substrate do not align in perfectly straight wires, but rather in bundles between and around the electrode tips. There is also a large difference between strings on glass and silicon substrate. On glass (fig. 4.7) most particles align in the gap between the electrodes, while on silicon (fig. 4.12) particles align between the electrodes, but also in small wires perpendicular to the electrodes. Since the particles move towards areas of higher field strength, these different movements show that the structure of the electric field is quite different on glass and on silicon, due to the conducting silicon layer.

Figure 4.9 shows simplified simulations of the behaviour of the electric field between and around the electrodes in the circular configuration. The simulations show the effect of having a conducting layer underneath the electrode pattern, and can give some hints to what is going on during alignment on the silicon substrate. In 4.9b the charged electrodes have induced a non-uniform charge distribution on the conductive backside of the silicon chip, modifying the electric field. Compared to 4.9a, which corresponds to the situation on glass substrate with no conducting layer underneath, the density of field lines is smaller in the gap, meaning that the field strength between the electrodes is reduced. During the alignment process it was shown that in this situation the field strength was not sufficiently high for complete strings to form. It is emphasised that the simulations are carried out using a static electric field, whereas the alternating field may induce even more modifications, through capacitive effects both between the electrodes and between electrodes and the silicon layer.

To solve the issue with capacitive effects, the silicon layer was connected to one of the electrodes during the alignment. This reduced the capacitive effects with a considerable amount, since the charges were no longer free to move around as they could when the layer was floating, and the field strength increased to a level where complete strings could be achieved. The field lines for this situation are illustrated in figures 4.9c and 4.9d, where the conducting layer is connected to the inner electrode and outer electrodes, respectively. The figures show that the field is altered and does no longer follow a straight line on top of the substrate between the electrodes, as it does in the simpler case in figure 4.9a. The more complex field still results in particles assembling between the electrodes, but they might be lifted from the substrate close to the electrode tips, which means no connection to the electrodes. Seen from above in a microscope the particles may still seem to be connected.

5.3 Electrical properties

Research on single strings from electric field alignment of CB [27] has shown that 1 out of 2 alignments results in strings with conductance of a few S/m. Alignment using electrodes in a circular configuration on glass substrate, as presented in this thesis, gave more promising results, with three out of seven different glass chips resulting in 15 conducting strings out of 15 possible, with resistances below 5 MΩ. Improvement of the process, by optimising field strength and alignment time, could

lead to even better statistics.

When 15 strings are aligned at the same time on the same substrate, using the same applied voltage, the conditions are equal for all 15 strings. Nevertheless, even under the very same conditions relatively large variations in resistance is observed, as seen from figure 4.14b. The resistance of the aligned CB strings is therefore quite random, and a sample with 15 strings with a uniform resistance is not possible to obtain.

Figure 4.15 shows the change of resistance of conducting strings on glass substrate after 3 and 10 weeks. Most strings undergo a change of 50 % or less during 10 weeks. When the resistance increases, it will affect the gauge factor and hence the sensitivity, as seen from equation 2.3. The sensitivity will be reduced with time, but at a slow pace. However, since it is the relative change in resistance that is detected during deflection, this will not considerably influence the strain sensing. Also, because of this, a variation in resistance of the strings is not a problem.

Measurements of current and phase angle were carried out for all the aligned CB strings, and also for homogeneous samples and polymer for comparison. Capacitive effects from the conducting silicon layer, which introduced modifications of the field during alignment, was also an issue when doing the electrical characterisation of strings on silicon substrate. It was found necessary to connect the silicon layer to ground to be able to measure any changes due to change in frequency and deflection. This might indicate that grounding of the silicon layer during the alignment process could eliminate the interfering capacitive effects, and give results similar to those on glass substrate.

In figure 4.18b the phase angle for isotropic 0.1 vol.% CB is stable at +90 degrees for low frequencies, which would imply an inductive behaviour instead of capacitive. Also, the phase angle for the isotropic 12 vol.% CB suddenly jumps from -90 to +90 degrees. This might imply that something is changing drastically in the polymer structure, or that the instrument does not properly separate between a phase angle and the same value shifted 180 degrees. When measuring the phase angle for a standard resistor, the result was a phase angle of -180, and for a standard capacitor it was -90, hinting that the latter explanation is more likely to be true. Due to the result for the resistor, all phase angles were shifted 180 degrees before plotting, so that the initial values for isotropic 0.1 vol.% CB was close to -90, meaning similar behaviour as the standard capacitor.

As seen from the phase angles in figures 4.17b and 4.18b, the strings show mostly a resistive effect, with phase angles close to zero (when shifted 180 degrees). However, since the phase angles are not exactly zero a capacitive effect might also be present. A simplified model to picture this may consist of a resistor and a capacitor in series, or the same elements in parallel, as shown in figures 5.1a and 5.1b, respectively. Figure 5.1c shows an arrangement of particles which could give capacitive and resistive effects corresponding to the model shown in figure 5.1b. In reality the situation is more complex, with resistive behaviour in each of the single particles that make up the string, as well as conductive behaviour between the particles.

Capacitance for each of the samples was calculated using the two different circuit

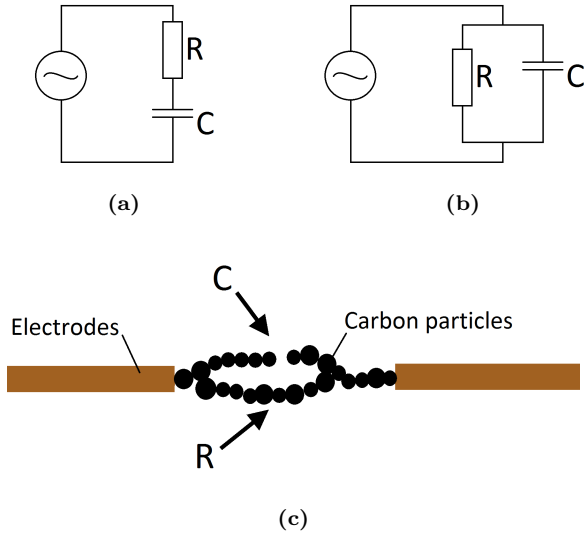

Figure 5.1: Electric circuit models for aligned CB particles. (a) Resistance and capacitance in series, (b) resistance and capacitance in parallel, and (c) a string of CB particles, forming a capacitor and a resistor in parallel.

models. Details are presented in appendix A. The calculated capacitance for the strings on glass and silicon substrate, from each of the two models, are shown in figure 5.2 and 5.3, respectively. Only measurements with current in the range of 0 - 1 μA are included.

Figure 4.18 shows that the aligned and non-conducting strings on silicon substrate behaves no differently than an empty electrode pattern on the same substrate. Above 7.2 kHz the current increases out of the range of 1 μA in both cases, which is clearly a result of capacitive effects in the electrode pattern, and not due to the CB strings. For comparison the capacitances for all strings on one silicon chip are shown in figure 5.4, as well as for the empty electrode pattern, showing that all strings on silicon substrate behave in a similar fashion.

The fact that the strings behaves just like the empty electrode pattern might indicate that the break in connection is between the string and the electrode tips, and not in the middle of the string, as suggested in figure 5.1c. If the gap leading to high resistances was somewhere on the string, rather than on both edges, the capacitance would be higher for the string than for the empty electrode pattern, since the gap distance would be much shorter. The electric field simulations also indicate that the CB strings might not be connected to the electrode tips, since the field does not follow a straigth line between the electrodes, as seen in the simulations in figures 4.9c and 4.9d. Bad connection between particles and electrodes are also reported by Park *et al.* [10]. They used carbon fibres as a piezoresistive element between the electrodes, and solved the issue by depositing Au on top of the fibres. This showed a 2-6 times reduction in resistance.

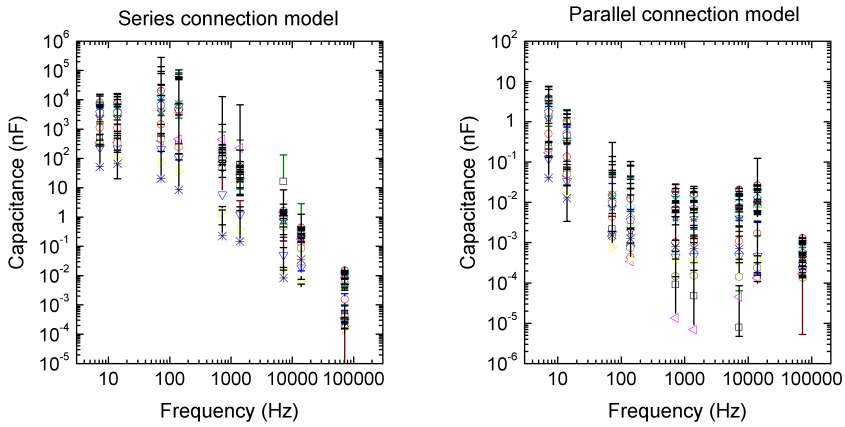

(a) **(b)**

Figure 5.2: Capacitance of CB strings on circular electrode pattern on glass substrate calculated using (a) a model of a capacitor and resistor in series and (b) a capacitor and resistor in parallel. Each symbol corresponds to different a string.

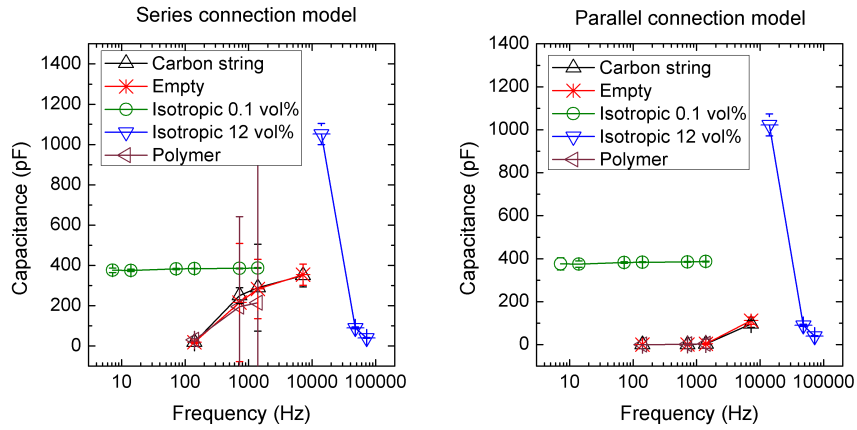

(a) **(b)**

Figure 5.3: Capacitance of CB strings on circular electrode pattern on silicon substrate calculated using (a) a model of a capacitor and resistor in series and (b) a model of a capacitor and resistor in parallel, for aligned CB string, empty electrode pattern, isotropic CB with 0.1 vol.% and 12.0 vol.%, and pure polymer (Dymax). The applied voltage was 10 mV for 12 vol.% CB, and 100 mV for the rest of the samples.

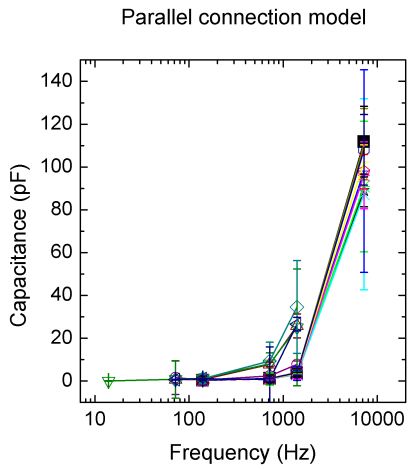

Figure 5.4: Capacitance of CB strings on circular electrode pattern on silicon substrate calculated using a model of a capacitor and resistor in parallel, showing all strings on one silicon substrate. The black square shows the calculated capacitance with no sample on the electrode pattern.

When modelling the CB string as a resistor and capacitor in series, capacitive effects are present already at a frequency of 1 kHz, as seen in figure 5.3a, which means that the alignment process could have been influenced by these effects. This suggests that a better alignment process could be achieved by reducing the frequency to 300 - 500 Hz. On the other hand, Dimaki and Bøggild [36] analysed the frequency dependence of dielectrophoretically aligned CNTs, and found that higher frequencies gave better alignment and lower resistance. If these results are transferable to CB particles the capacitive effects resulting from the conducting silicon layer should be eliminated by other means than reducing the frequency, to avoid a loss in alignment ability.

The isotropic dispersion with 0.1 vol.% CB shows capacitive behaviour on the frequency range where currents below 1 µA could be measured, and the capacitance is higher compared to the empty pattern and CB string on silicon substrate using both models, as seen in figure 5.3. This means that aligned CB strings that seem to be conducting, but in reality has a gap between the string and the electrodes, are less effective than an isotropic dispersion with the same filler content in terms of capacitive effects.

For the 12 vol.% dispersion the current starts out above the range of 1 µA, and decreases below this value after 14 kHz. High current at low frequencies indicates that there are percolating networks through the sample, with sufficient conductance to let a current go through. Percolating networks at a filler content of 12 vol.%, a value that is considerably lower than the theoretical value of 16 vol.% for a homogeneous dispersion, supports the results from Flandin *et al.* [6], which showed that the electric charge on the particles shifts the percolation threshold. They

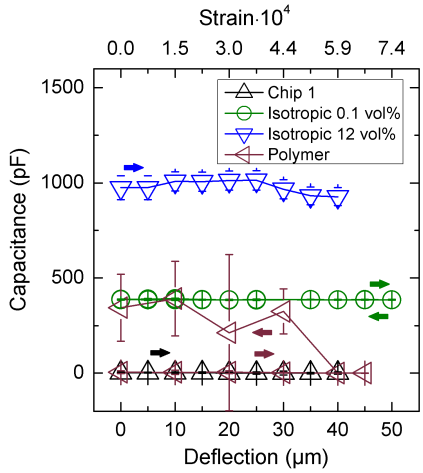

Figure 5.5: Capacitance as a function of deflection on circular electrode pattern for aligned string (Chip 1), isotropic CB with 0.1 vol.% and 12.0 vol.% and pure polymer (Dymax).

found the percolation threshold of CB particles to be close to 0.9 vol.%.

5.4 Electromechanical properties

Strain measurements were done by measuring the current and phase angle through the aligned CB strings while bending the sample. To avoid capacitive effects from the conducting silicon layer, the chip was connected to ground through the metal holder.

An abrupt change in current and phase angle for the pure polymer is observed on the return of the micrometer screw, seen in figure 4.20, which can be attributed to a break in connection between ground and the conducting silicon layer of the chip. The same argument can explain the behaviour of the aligned CB string on chip 2 in figure 4.20c. When bringing the micrometer screw back during deflection, the current makes a jump, and ends up at a value which is much higher than the initial value for the current. This could also be due to breaking of the connection to ground, and as a result capacitive effects in the conducting silicon layer leads to a higher current. A lost connection to ground can also explain the sudden jump at 25 µm deflection. Here the connection to ground seems to be restored, since the current suddenly drops again.

No significant change is observed for current or phase angle for the isotropic 0.1 and 12 vol.% CB in figure 4.20. The different phase angle for the two samples, of +90 and -90 degrees, respectively, can be explained by the instrumentation, as discussed on page 40. For both aligned CB strings on silicon substrate the current decreases slightly as a function of deflection, to about 10-20 % of the initial value,

as seen in figure 4.20c.

The corresponding capacitance for the deflection measurements were calculated using the parallel connection model discussed earlier, with calculations from section A.2 in appendix A. The calculated values are shown in figure 5.5, with samples corresponding to those in figure 4.20. Values for the resistance of each sample was calculated as well, but are not presented here. To give an idea about the sensitivity of the aligned strings in terms of strain sensing, the relative change in resistance as a function of deflection was calculated for the two strings in figure 4.20c, as well as for the isotropic 0.1 vol.% CB sample.

The aligned strings on chip 1 and chip 2 showed a relative change in resistance, $\Delta R/R$, of 10.13 and 0.596, respectively, while the relative change in resistance for the isotropic 0.1 vol.% CB was 0.005. The very high value of 10.13 for the string on chip 2 is explained by the sudden change in phase angle at 30 µm deflection, seen in figure 4.20b. This might be caused by interferences in the connection to ground giving capacitive effects. The change in capacitance can be seen by downscaling figure 5.5, as done in figure 5.6. The large error bars indicate that the error is too large to give an accurate estimate of the relative change in resistance. Consequently, the data is too thin to calculate the gauge factor, given by equation 2.3.

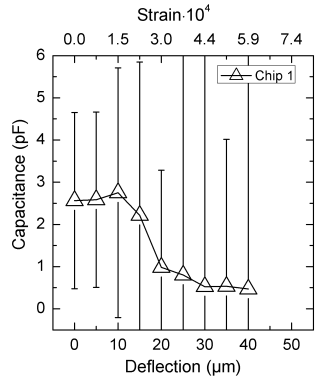

Figure 5.6: Calculated capacitance for aligned string on silicon chip 1.

Both substrates with the aligned CB strings broke before any more measurements could be done. However, apart from the big jump at 25 µm for chip 2, which can be explained by a break in the connection to ground, both samples behave in a similar manner, and a decrease in current of 80-90 % is promising in terms of sensing applications.

Chapter 6

Conclusion and future work

This study has shown the parallel integration of multiple aligned CB strings in a two-dimensional geometry. With some improvements of the materials and alignment process this has implications towards sensor applications. The use of CB gives lower production costs than e.g. CNTs, and the lower filler content that is required with the alignment process makes sure that the mechanical properties of the flexible polymer matrix are maintained.

Alignment of CB particles using the circular electrode configuration on glass substrate were studied first. In three out of seven samples, with 15 electrode pairs on each sample, the result was 100 % formation of strings with electrical connection, with all 15 strings showing a resistance below 5 MΩ. In the other four samples, a total of 38 % of the strings showed a resistance below 5 MΩ. The field strength was varied slightly from sample to sample, so only small variations made the difference between a few connected strings and 100 % string formation. Optimisation of the parameters, such as field strength and alignment time, could lead to even better results.

The alignment was then studied on silicon substrate. During the alignment the conducting silicon layer of the substrate modified the electric field in a way that CB strings were grown, but without any electrical connection. Also, when bending the substrate, capacitive effects due to the silicon layer influenced the measurements. Connecting the conducting layer to ground proved to be a good solution during the bending process, as long as the connection was maintained through the whole process.

In addition to removing capacitive effects during impedance measurements, grounding the silicon layer could also improve the alignment process, since the capacitive effects would be eliminated and the electric field would still be sufficiently uniform along the substrate between the electrodes. This might lead to better contact between the strings and the electrodes. If grounding of the silicon layer does not work, then other substrates, e.g. elastomers, should be considered as a substitute for the silicon substrate.

Bending measurements showed that even for a non-conducting string a change in current was observed as a function of deflection, and the initial current was

reduced by 80-90% with a deflection of 35 µm. With a conducting string, the change in resistance could be measured as a function of deflection, and the 2D electrode pattern with aligned strings could potentially work as a strain sensor.

Future work could, with some alterations of the procedure, most likely result in conducting strings on a substrate with the circular electrode pattern. Successful alignment on glass substrate shows that by eliminating the capacitive effects from the conducting silicon layer, while still maintaining a sufficiently strong and uniform electric field between the electrodes, well-aligned and conducting strings would be formed between the electrode tips. These strings could then be studied further using the same bending setup, while monitoring the change in resistance as a function of deflection.

Appendix A

Electric circuit calculations

The impedance of a resistor and capacitor is given by $Z_R = R$ and $Z_C = 1/(i\omega C)$, respectively, where R is the resistance, ω is the angular frequency, C is the capacitance and $i = \sqrt{-1}$. The reactance of a capacitor, X_C, is a measure of how the capacitor opposes the flow of electricity, and is equal to $1/(\omega C)$, i.e. the absolute value of the impedance. When the current $I = V/Z$ and phase angle ϕ of the system are measured, the resistance R and capacitance C can be found from the following calculations. [37]

A.1 Resistor and capacitor in series

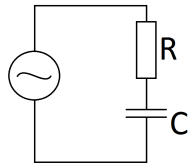

Figure A.1: Resistance and capacitance in series.

The total impedance for electrical components in series connection is equal to the sum of the impedance of each component. For a resistor and capacitor in series, as shown in figure A.1, the total impedance will be:

$$Z = Z_R + Z_C = R + \frac{1}{i\omega C}, \tag{A.1}$$

i.e. the resistance will be the component of the impedance along the real axis, while the capacitor reactance will be the component along the imaginary axis. The phase angle ϕ is the angle between the total impedance and the real axis, giving:

$$Z_R = Z\cos\phi \Rightarrow \underline{R = Z\cos\phi}, \tag{A.2}$$

$$Z_C = Z \sin\phi \Rightarrow \underline{C = \frac{1}{\omega Z \sin\phi}}. \tag{A.3}$$

A.2 Resistor and capacitor in parallel

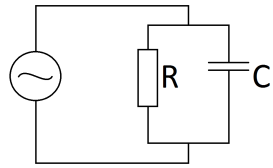

Figure A.2: Resistance and capacitance in parallel.

Method I The total impedance for a resistor and capacitor in parallel, shown in figure A.2, is given by:

$$\frac{1}{Z} = \frac{1}{Z_R} + \frac{1}{Z_C}. \tag{A.4}$$

Rewriting, and inserting $Z_R = R$ and $Z_C = 1/(\omega C)$ gives:

$$Z = \frac{1}{\frac{1}{R} + i\omega C} = \frac{R - i\omega C R^2}{1 + (\omega C R)^2}. \tag{A.5}$$

Again, Z_R is the component of the total impedance along the real axis, and Z_C is the component along the imaginary axis, giving:

$$Z_R = Z \cos\phi = \frac{R}{1 + (\omega C R)^2}, \tag{A.6}$$

$$Z_C = Z \sin\phi = \frac{\omega C R^2}{1 + (\omega C R)^2}. \tag{A.7}$$

Dividing equation A.7 with equation A.6, and solving for R and C gives:

$$\underline{R} = Z \cos\phi \cdot (1 + \tan^2\phi) = \underline{\frac{Z}{\cos\phi}}, \tag{A.8}$$

$$\underline{C} = \frac{\tan\phi}{\omega R} = \underline{\frac{\sin\phi}{\omega Z}}. \tag{A.9}$$

Method II In a parallel RC circuit, the total current will at any time be equal to the sum of the current through each component, i.e.

$$I = I_R + I_C. \tag{A.10}$$

A phasor diagram of the situation is shown in figure A.3. From the phasor diagram it is evident that $I_R = I\cos\phi$ and $I_C = I\sin\phi$. Since the impedance is equal to the ratio between the voltage and the current through the component, we get:

$$Z_R = \frac{V}{I_R} = \frac{V}{I\cos\phi} = \frac{Z}{\cos\phi} \Rightarrow \underline{R = \frac{Z}{\cos\phi}}, \tag{A.11}$$

$$Z_C = \frac{V}{I_C} = \frac{V}{I\sin\phi} = \frac{Z}{\sin\phi}, \tag{A.12}$$

$$\Rightarrow \underline{C} = \frac{1}{\omega|Z_C|} = \underline{\frac{\sin\phi}{\omega Z}}. \tag{A.13}$$

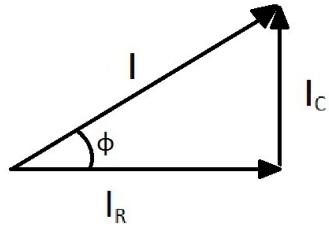

Figure A.3: Phasor diagram for current of a resistor and a capacitor in parallel.

Bibliography

[1] R. Pethig. Review article—dielectrophoresis: Status of the theory, technology, and applications. *Biomicrofluidics*, 4(2):022811–35, 2010.

[2] M. Knaapila, J. P. Pinheiro, M. Buchanan, A. T. Skjeltorp, and G. Helgesen. Directed assembly of carbon nanocones into wires with an epoxy coating in thin films by a combination of electric field alignment and subsequent pyrolysis. *Carbon*, 49:3171–3178, 2011.

[3] M. Knaapila, H. Høyer, E. Svasand, M. Buchanan, A. T. Skjeltorp, and G. Helgesen. Aligned carbon cones in free-standing uv-curable polymer composite. *J. Polym. Sci., Part B: Polym. Phys.*, 49:399–403, 2011.

[4] M. Knaapila, O. T. Romoen, E. Svasand, J. P. Pinheiro, O. G. Martinsen, M. Buchanan, A. T. Skjeltorp, and G. Helgesen. Conductivity enhancement in carbon nanocone adhesive by electric field induced formation of aligned assemblies. *ACS Appl. Mater. Interfaces*, 3:378–384, 2011.

[5] T. Prasse, L. Flandin, K. Schulte, and W. Bauhofer. In situ observation of electric field induced agglomeration of carbon black in epoxy resin. *Applied Physics Letters*, 72(22):2903–2905, 1998.

[6] L. Flandin, T. Prasse, R. Schueler, K. Schulte, W. Bauhofer, and J. Y. Cavaille. Anomalous percolation transition in carbon-black-epoxy composite materials. *Physical Review B*, 59(22):14349–14355, 1999. PRB.

[7] T. Prasse, M.-K. Schwarz, K. Schulte, and W. Bauhofer. The interaction of epoxy resin and an additional electrolyte with non-oxidised carbon black in colloidal dispersions. *Colloids and Surfaces A: Physicochemical and Engineering Aspects*, 189(1-3):183–188, 2001.

[8] A. Sharma, C. E. Bakis, and K. W. Wang. A new method of chaining carbon nanofibers in epoxy. *Nanotechnology*, 19(Copyright (C) 2012 American Chemical Society (ACS). All Rights Reserved.):325606/1–325606/5, 2008.

[9] C.-S. Lim, A. J. Rodriguez, M. E. Guzman, J. D. Schaefer, and B. Minaie. Processing and properties of polymer composites containing aligned functionalized carbon nanofibers. *Carbon*, 49(6):1873–1883, 2011.

[10] C. S. Park, B. S. Kang, D. W. Lee, T. Y. Choi, and Y. S. Choi. Fabrication and characterization of a pressure sensor using a pitch-based carbon fiber. *Microelectronic Engineering*, 84(5-8):1316–1319, 2007.

[11] R. J. Grow, Q. Wang, J. Cao, D. Wang, and H. Dai. Piezoresistance of carbon nanotubes on deformable thin-film membranes. *Applied Physics Letters*, 86(9):093104–3, 2005.

[12] T. Helbling, C. Roman, L. Durrer, C. Stampfer, and C. Hierold. Gauge factor tuning, long-term stability, and miniaturization of nanoelectromechanical carbon-nanotube sensors. *Electron Devices, IEEE Transactions on*, 58(11):4053–4060, 2011.

[13] Alamusi, N. Hu, H. Fukunaga, S. Atobe, Y. Liu, and J. Li. Piezoresistive strain sensors made from carbon nanotubes based polymer nanocomposites. *Sensors*, 11(11):10691–10723, 2011.

[14] D. W. H. Fam, Al Palaniappan, A. I. Y. Tok, B. Liedberg, and S. M. Moochhala. A review on technological aspects influencing commercialization of carbon nanotube sensors. *Sensors and Actuators B: Chemical*, 157(1):1–7, 2011.

[15] M. H. G. Wichmann, S. T. Buschhorn, J. Gehrmann, and K. Schulte. Piezoresistive response of epoxy composites with carbon nanoparticles under tensile load. *Physical Review B*, 80(24):245437, 2009. PRB.

[16] M. Knite, V. Teteris, A. Kiploka, and J. Kaupuzs. Polyisoprene-carbon black nanocomposites as tensile strain and pressure sensor materials. *Sensors and Actuators A: Physical*, 110(1-3):142–149, 2004.

[17] L. Gammelgaard, P. A. Rasmussen, M. Calleja, P. Vettiger, and A. Boisen. Microfabricated photoplastic cantilever with integrated photoplastic/carbon based piezoresistive strain sensor. *Applied Physics Letters*, 88(11), 2006.

[18] C. Cochrane, V. Koncar, M. Lewandowski, and C. Dufour. Design and development of a flexible strain sensor for textile structures based on a conductive polymer composite. *Sensors*, 7(4):473–492, 2007.

[19] H. Høyer, M. Knaapila, J. Kjelstrup-Hansen, X. Liu, and G. Helgesen. A strain sensor based on an aligned carbon particle string in a uv-cured polymer matrix. *Appl. Phys. Lett.*, 99:213106/1–213106/3, 2011.

[20] H. Høyer, M. Knaapila, J. Kjelstrup-Hansen, X. Liu, and G. Helgesen. Individual strings of conducting carbon cones and discs in a polymer matrix: Electric field-induced alignment and their use as a strain sensor. *J. Polym. Sci., Part B: Polym. Phys.*, 50:477–483, 2012.

[21] J. S. Wilson. *Sensor Technology Handbook*. Elsevier Science & Technology, Saint Louis, MO, USA, 2004.

[22] S. Franssila. *Introduction to Microfabrication (2nd Edition)*. Wiley, Hoboken, NJ, USA, 2010.

[23] Condalign. `www.condalign.no`. (19.11.12).

[24] P. A. Smith, C. D. Nordquist, T. N. Jackson, T. S. Mayer, B. R. Martin, J. Mbindyo, and T. E. Mallouk. Electric-field assisted assembly and alignment of metallic nanowires. *Applied Physics Letters*, 77(9):1399–1401, 2000.

[25] A. Nocke, M. Wolf, H. Budzier, K.-F. Arndt, and G. Gerlach. Dielectrophoretic alignment of polymer compounds for thermal sensing. *Sensors and Actuators A: Physical*, 156(1):164–170, 2009.

[26] B. R. Burg, T. Helbling, C. Hierold, and D. Poulikakos. Piezoresistive pressure sensors with parallel integration of individual single-walled carbon nanotubes. *Journal of Applied Physics*, 109(6):064310–064310–6, 2011.

[27] H. Høyer. Individual strings of conducting carbon particles in polymer matrix: Electric field induced preparation and electromechanical properties. Master's thesis, Norwegian University of Science and Technology, 2011.

[28] International Carbon Black Association. `http://www.carbon-black.org/what_is.html`. (08.10.12).

[29] Alfa Aesar. `www.alfa.com`. (08.10.12).

[30] H. A. Pohl. The motion and precipitation of suspensoids in divergent electric fields. *J. Appl. Phys.*, 22:869–71, 1951.

[31] S. D. Senturia. *Microsystem Design*. Kluwer Academic Publishers, Hingham, MA, USA, 2000.

[32] J. Kjelstrup-Hansen, NanoSYD. Personal communication, November 2012.

[33] Lindberg & Lund AS. `http://www.lindberg-lund.no`. (08.10.12).

[34] NanoSYD, Mads Clausen Institute, University of Southern Denmark. `http://www.sdu.dk/en/Om_SDU/Institutter_centre/Mci_mads_clausen`. (08.10.12).

[35] Physics Software. `http://www.physics-software.com/software.html`. (30.11.12).

[36] M. Dimaki and P. Bøggild. Frequency dependence of the structure and electrical behaviour of carbon nanotube networks assembled by dielectrophoresis. *Nanotechnology*, 16(6):759, 2005.

[37] N. Storey. *Electronics : A Systems Approach*. Pearson Prentice Hall, Harlow, 2009. 4th ed.